Geochemistry
Geophysics
Geosystems
G^3
AN ELECTRONIC JOURNAL OF THE EARTH SCIENCES
Published by AGU and the Geochemical Society

Article
Volume 3, Number 11
23 November 2002
1070, doi:10.1029/2001GC000225
ISSN: 1525-2027

O_2 volumes at high pressure from $KClO_4$ decomposition: D'' as a siderophile element pump instead of a lid on the core

D. Walker
Lamont-Doherty Earth Observatory of Columbia University, Palisades, New York 10964, USA
(dwalker@ldeo.columbia.edu)

S. M. Clark
Daresbury Laboratory, CLRC, Warrington WA4 4AD, UK

Advanced Light Source, LBNL, MS 80-101, 1 Cyclotron Road, Berkeley, California 94720, USA

L. M. D. Cranswick
Lamont-Doherty Earth Observatory of Columbia University, Palisades, New York 10964, USA

Daresbury Laboratory, CLRC, Warrington WA4 4AD, UK

Department of Crystallography, Birkbeck College, University of London, Malet Street, Bloomsbury, London, WCIE 7HX, UK

M. C. Johnson
Department of Geography and Environmental Engineering, United States Military Academy, West Point, New York 10996, USA

R. L. Jones
Daresbury Laboratory, CLRC, Warrington WA4 4AD, UK

[1] New measurements of the high-pressure volume of oxygen make plausible old, controversial diamond anvil cell (DAC) observations of a high-pressure reaction between liquid Fe and Fe-bearing silicate in which FeO dissolved into liquid Fe. If the Earth's D'' layer between core and mantle is the waste product of this reaction proceeding forward with oxygen transfer to the core, then D'' would form an effective lid preventing escape of siderophile elements from the core. On the other hand, it is at least as plausible that the core is now oxygen saturated and that core cooling and internal crystallization drive this reaction backward with transfer of Fe- and O-rich material out of the core into D''. The ^{186}Os anomalies in some plume basalts are more consistent with this D'' as a siderophile element pump scenario than the D'' as-lid scenario. Contributions of siderophile elements to the mantle from the core could assist in balancing the persistently enigmatic budget of these elements.

Components: 11,783 words, 8 figures, 3 tables.

Keywords: Oxygen volume; high-pressure; D"; core evolution; potassium perchlorate.

Index Terms: 1015 Geochemistry: Composition of the core; 3630 Minerology and Petrology: Experimental minerology and petrology; 3919 Mineral Physics: Equations of the state; 8125 Tectonophysics: Evolution of the Earth.

Received 4 September 2001; **Revised** 14 July 2002; **Accepted** 17 July 2002; **Published** 23 November 2002.

Walker, D., S. M. Clark, L. M. D. Cranswick, M. C. Johnson, and R. L. Jones, O_2 volumes at high pressure from $KClO_4$ decomposition: D″ as a siderophile element pump instead of a lid on the core, *Geochem. Geophys. Geosyst.*, *3*(11), 1070, doi:10.1029/2001GC000225, 2002.

1. Introduction

[2] *Knittle and Jeanloz* [1989a, 1991] reported that molten iron metal in a diamond anvil cell (DAC) reacts at pressures greater than 300 kbar with Fe-bearing perovskite to give, upon quench, Fe-poor perovskite, stishovite, iron metal, iron silicide, and wüstite. Presumably the FeO and possibly the FeSi were in solution in the molten iron at P,T and formed by exsolution and crystallization during quench. If the FeO were not in the Fe alloy solution at high P,T then Fe-bearing perovskite melting products should include wüstite. Partial melting studies of Fe-bearing perovskite, however, have not reported wüstite [*Heinz and Jeanloz*, 1987; *Knittle and Jeanloz*, 1989b; *Zerr and Boehler*, 1993]. In fact, the driving force for the reaction is claimed to be the solution of FeO into the molten alloy. *Goarant et al.* [1992] confirmed the observations of *Knittle and Jeanloz* [1989a, 1991] on the nature and identity of the reaction products. They extended the observations to a variety of silicate bulk compositions, with and without sulfide. *Goarant et al.* [1992] also emphasized the importance of oxygen solution in molten iron by identifying the following end-member reaction as the underlying motivator of the observed transformations.

$$^{\text{silicate/oxide}}\text{FeO} = {}^{\text{liq}}\text{Fe} + {}^{\text{liq}}\text{O} \qquad (1)$$

[3] The DAC observations from two laboratories agree that the reactions observed proceed at high pressure. But reaction (1) proceeding forward at high pressure is very difficult to reconcile with current estimates of the volumes involved. Figure 1 shows the molar volume for two-atom moles of material along the join 2Fe-O_2 at 300 kbar, 2500°C, a nominal condition for the equilibrium of reaction (1). The volume of crystalline FeO ($^{\text{Wüs}}\overline{\text{V}}$) is extrapolated from several sources [*Hazen and Jeanloz*, 1984; *Yagi et al.*, 1985; *Fei et al.*, 1992]. (Note here, a leading superscript denotes the phase whereas a trailing subscript denotes a component. When Wüs is used as a trailing subscript it indicates the composition of wüstite whether or not it is exactly FeO and whether or not it is in the crystalline wüstite phase. Thus, for example, $^{\text{L}}\overline{\text{V}}_{\text{Wüs}}$ is the partial molar volume that the oxide has in the liquid metal.) The volume of liquid 2Fe is based upon the volume of crystalline Fe [*Boehler et al.*, 1990] with a generic ΔV of melting of 4%. The currently accepted volumes of supercritical liquid O_2 in Figure 1a are derived from molecular dynamics models [*Belonoshko and Saxena*, 1991]. They are consistent with the shock wave measurements [*Wackerle et al.*, 1968; *Nellis and Mitchell*, 1980; *Ross and Ree*, 1980] on which they are partially based. They also are consistent with new impulsively stimulated scattering (ISS) measurements [*Abramson et al.*, 1999].

[4] Reaction (1) describes the solubility of FeO in liquid metal alloy. To understand whether FeO solubility is expected to increase or decrease with pressure, consider Figure 2. The melting relations in system Fe-O are given schematically at a lower pressure P_1, and a higher pressure P_2. At some fixed $^{\text{L}}X_{O_2}$ (the fraction of O_2 in liquid metal) along the saturation curve with "FeO," the solubility increases at P_2 if the temperature of exsolution of "FeO" is lower than at P_1. (The solvus shrinks as solubility increases as shown hypothetically in Figure 2.) The saturation can be with crystalline FeO, liquid FeO saturated with liquid metal, or FeO in solution in some oxide or silicate without affecting this analysis, other than by adding additional corrections for solution effects. For simplicity, assume P is high enough that wüstite is the phase saturating the liquid metal.

$$\left.\frac{\partial \text{T}}{\partial \text{P}}\right|_{^{\text{L}}X_{O_2},\text{L=Ox}} = \frac{^{\text{L}}\bar{\text{V}}_{\text{Wüs}} - {}^{\text{Wüs}}\bar{\text{V}}}{^{\text{L}}\bar{\text{S}}_{\text{Wüs}} - {}^{\text{Wüs}}\bar{\text{S}}} = \frac{\Delta \text{V}_{\text{R}}}{\Delta \text{S}_{\text{R}}}$$

[5] For fixed $^{\text{L}}X_{O_2}$ on the saturation curve of liquid metal with oxide (L = Ox), the equation above gives the variation of T with P sought (derivation

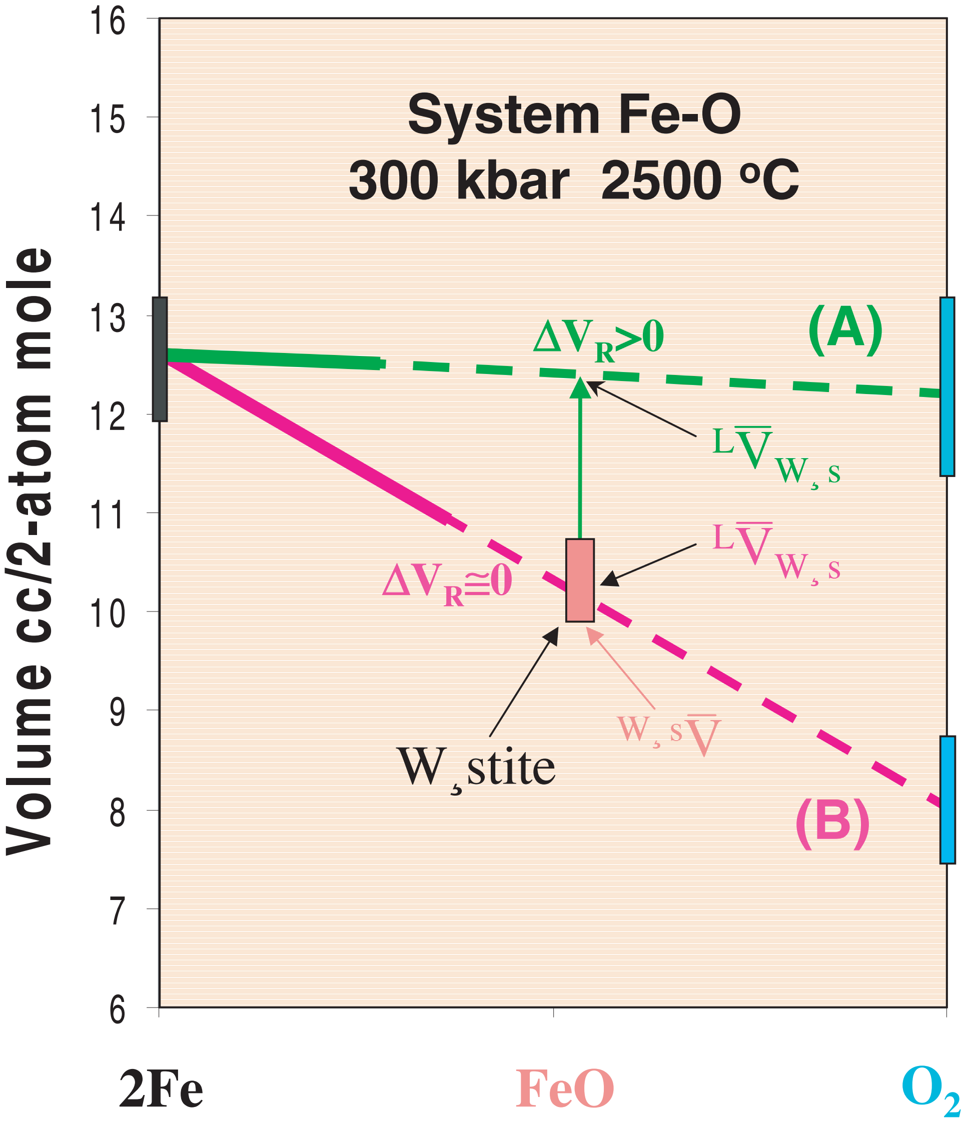

Figure 1. Volume–composition relations in system Fe-O at high pressure and temperature. Volumes of liquid metal solutions are approximated as linear mixtures of liquid 2Fe and fluid O_2. Choice of two-atom, molar units facilitates graphical presentation. The linear approximation is likely to give minimum estimates for ${}^{L}\overline{V}_{Wüs}$. Even so, the use of the conventionally accepted values for O_2 volume gives $\Delta V_R = ({}^{L}\overline{V}_{Wüs} - {}^{Wüs}\overline{V}) > 0$ as shown in part (a). This means that little FeO would be expected to dissolve in liquid Fe metal at these P-T conditions. Part (b) shows the volumes of liquid metal solutions for O_2 volumes indicated in the present study. O_2 EOS parameters from Figure 8 and Table 1 are used to extrapolate to the 300 kbar, 2500°C conditions of this figure. The extrapolation is fairly insensitive to the choices of EOS parameters. Direct fits to the data points of Figure 8 instead of the smoothed EOS give a change in oxygen volume of only from 7.9 to 8.2 cm^3/mol. (K_o changes from 121 to 312 kbar while K'_o changes from 11.4 to 6.4 for the different fitting procedures.) For O_2 volumes used in (b), $\Delta V_R \cong 0$, and appreciable solution of FeO in liquid metal is expected at higher pressures. 300 kbar is roughly the pressure found by *Knittle and Jeanloz* [1991] to mark the transition between reaction (1) proceeding or not, consistent with (b).

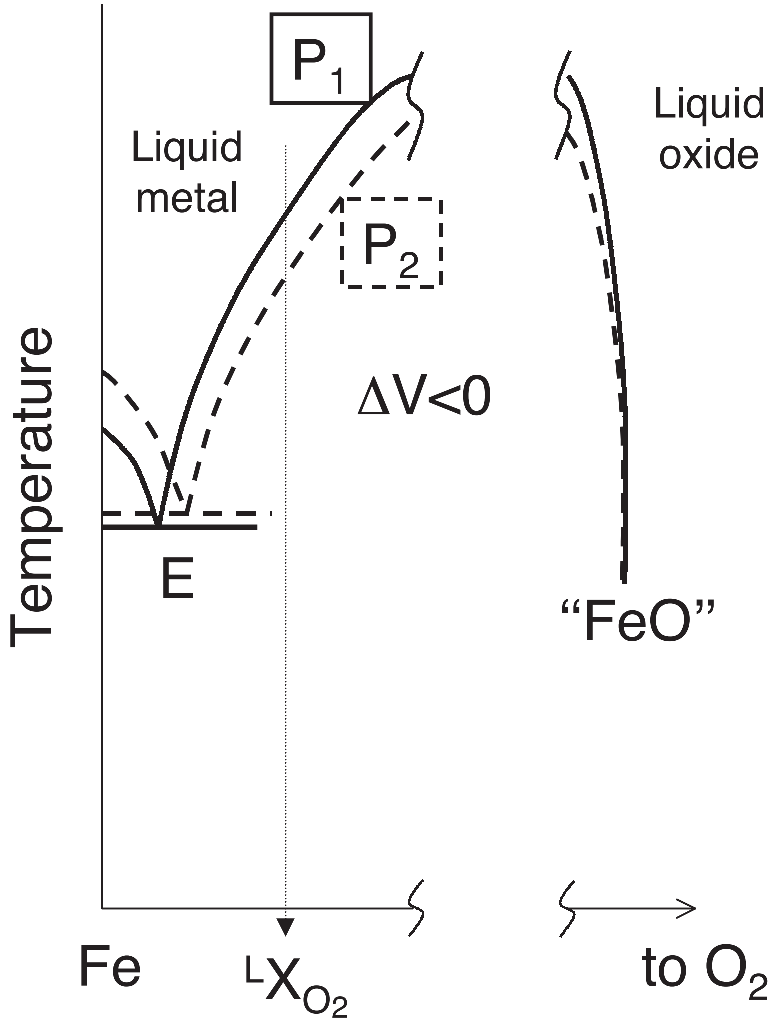

Figure 2. Temperature versus composition relations in Fe-O at two pressures. P_2 is higher than P_1. Eutectic liquid metal *E* forms between crystalline metal and liquid oxide (or solid oxide or Fe-bearing silicate depending in P-T-X investigated). The situation shown is for $\Delta V_R < 0$ corresponding to increased solubility of FeO in liquid metal with increasing pressure.

after *Walker et al.* [1988]). $^L\overline{V}_{Wüs}$ is approximated in Figure 1 for ideal volume mixing in metallic liquid as the volume at wüstite composition on the line connecting liquid Fe with fluid O_2. If $^L\overline{V}_{Wüs} > {}^{Wüs}\overline{V}$, ($\Delta V_R >$ O, as in Figure 1a), then $\partial T/\partial P >$ O for well-behaved entropies. Solubility is expected to decrease with pressure. For what pressures is this true, if any, is highly controversial even at low and moderate pressure. This controversy is well typified by the first order discrepancy between the results of *Ohtani et al.* [1984] and *O'Neill et al.* [1998]. If the volume relations of Figure 1a are correct then very little O_2 can dissolve into the liquid outer core because O_2 solubility in liquid metal is very low at low pressures and this analysis suggests that the solubility becomes even lower with increasing pressure. (The analysis is more complex if one tracks the eutectic composition *E* in Figure 2 with pressure. The position of *E* with pressure depends on the properties of all three phases: crystalline Fe metal, metallic liquid, and oxide. It is theoretically possible (but not especially plausible in the absence of detailed phase information) to have the solubility of O_2 in liquid metal increase, in the sense we have been considering, at the same time the eutectic composition *E* shifts to more O_2-poor compositions.)

[6] To determine whether reaction (1) is favored to proceed with increasing pressure or if the reverse reaction is favored, the molar volume of crystalline "FeO," $^{\text{Wüs}}\overline{V}$, must be compared to the partial molar volume of "FeO" in liquid metal, $^{L}\overline{V}_{\text{Wüs}}$. If ΔV_R for the comparison is positive, increasing the pressure will not drive the reaction. Using choice A in Figure 1, the current conventional wisdom, $\Delta V_R > O$ and the DAC observations can not be correct unless unprecedented solution effects of additional components and phases are invoked. *Knittle and Jeanloz* [1991] attempted to finesse this problem with the calculation of a more complex reaction than (1) using all the phases observed upon quench. $\Delta V_R < O$ was claimed, as required for consistency with the results they reported. Crystalline wüstite and iron silicide volumes, however, are not relevant to the calculation as these quench-produced phases are unlikely participants in the reaction as anything other than solution components in the liquid alloy. Because the calculation was not based on the partial molar properties of liquid alloy but upon the substitution of $^{\text{Wüs}}\overline{V}$ for $^{L}\overline{V}_{\text{Wüs}}$, the volume problem seen in Figure 1a is obscured. *O'Neill et al.* [1998] may be the only previous investigators to have noticed the apparent volume problem with the DAC results of Knittle and Jeanloz or Goarant et al., although they couched their objection in rather different terms.

[7] One may object that a linear volume interpolation between liquid 2Fe and O_2 does not rigorously capture $^{L}\overline{V}_{\text{Wüs}}$ in Fe alloy liquid. Indeed we would be very surprised if these fluids did mix ideally, however the linear graphical estimate of $^{L}\overline{V}_{\text{Wüs}}$ used in Figure 1 forms a reasonable lower bound on fluid volume. If the results of *O'Neill et al.* [1998] are included, the line would become an arch and ΔV_R would become even more positive. Even without the real curvature on volumes, which the liquid mixture probably has, the volumes of crystalline and liquid FeO of Figure 1a are clearly not compatible with much FeO solubility in liquid metal alloy. Low solubility has been reported up to 250 kbar by *Ito et al.* [1995] and by *O'Neill et al.* [1998]. But what if the difference between crystalline FeO, $^{\text{Wüs}}\overline{V}$, and liquid FeO partial molar volumes, $^{L}\overline{V}_{\text{Wüs}}$, changes sign at pressures above 300 kbar as implicitly required by *Knittle and Jeanloz* [1991] in their Figure 2? To reconcile the DAC observations with a diagram such as our Figure 1, the phase volume estimates need to change appreciably for such a sign change to occur. This change is unlikely for FeO and pure liquid Fe. The lower estimate for oxygen volume shown as Figure 1b, however, is based upon new $KClO_4$ decomposition results that differ considerably from the values of Figure 1a. These new determinations give oxygen volumes similar to our recent determinations based upon the decomposition of $KClO_3$ [*Johnson et al.*, 1997, 2001] and $RbClO_4$ [*Walker et al.*, 2001]. And they are consistent with ΔV_R having dropped to zero near 300 kbar as required by the DAC results.

2. Measurement of Solid Phase Volumes

[8] *Johnson et al.* [1997, 2001] measured high-pressure O_2 volumes indirectly by tracking the thermal decomposition of rhombohedral (R) $KClO_3$ from 29 to 76 kbar. Decomposition products are B2 KCl and O_2 gas through an intermediate stage of B2 KCl and orthorhombic (O) $KClO_4$. Crystalline volumes were measured at high P-T by in situ energy-dispersive X-ray diffraction (EDXRD) using the cubic/octahedral multianvil device in Station 16.4 of the Daresbury synchrotron radiation source [*Clark*, 1996]. Because the $\partial T/\partial P$ slope of the decomposition reaction was close to zero, the Clausius−Clapeyron equation simplifies and ΔV_R is about zero regardless of ΔS_R. O_2 volume was calculated as the difference between R $KClO_3$ and B2 KCl volumes along the high P-T decomposition curve. Because the oxygen volumes calculated were so different from the molecular dynamics, shock wave, and ISS values on which Figure 1a is based, we sought to improve our measurement procedures to either confirm or revise our initial efforts. First we devised a more comprehensive calibration procedure [*Walker et al.*, 2000] for the new three-element energy-dispersive detector on Station 16.4 SRS Daresbury [*Barnes et al.*, 1998]. Second, we devised more favorable sample illumination geometry for minimizing temperature gradient effects (Figure 3). And third, we inves-

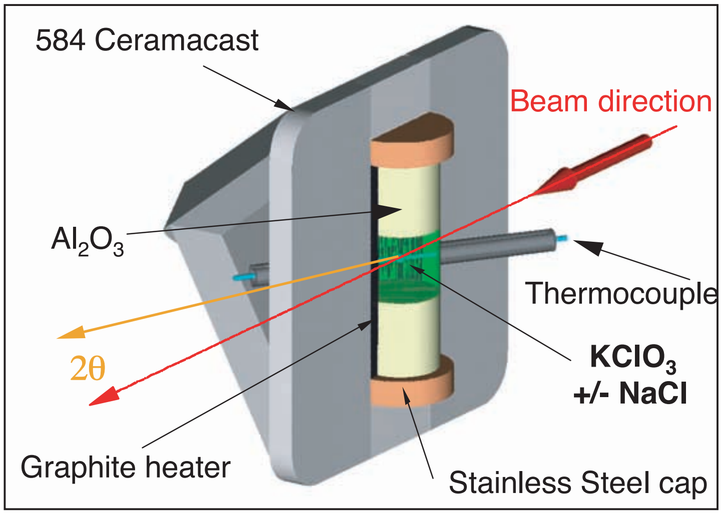

Figure 3. Assembly used for on-line experiments at Daresbury Lab Station 16.4 at high pressure and temperature with eight 12 mm TEL tungsten carbide anvils. Press compression axis and X-ray beam are both horizontal and intersect one another at an angle of 35°16′. Energy-dispersive X-ray detector has the plane of 2θ variation vertical as a result. With one exception, all runs had NaCl above the thermocouple and KCl or $KClO_3$ below the thermocouple. The exception was the experiment of 27 April 1998 [experiments r34227 and following at 2000 kN] in which only $KClO_3$ was present. This run was further exceptional in having the axis of the heater running from face to face of the octahedron rather than fin to fin as shown here.

tigated the stable, independent $KClO_4$ decomposition reaction as a crosscheck on our reinvestigation of the metastable $KClO_3$ decomposition. To anticipate our conclusion, we confirm the results of our earlier studies. We have had additional incentive to carefully reexamine our technique because of the adverse reaction of several reviewers to our considered suggestion that our measurements ought to be taken at least as seriously as the shock wave results. We present here these doubly reconsidered new results even knowing that two out of three reviewers at *Science* believes them to be dangerous nonsense, from which the community deserves protection, because these new results disagree with the dynamical techniques.

[9] Figure 3 shows the sample geometry used in 12 mm TEL assemblies. X-ray illumination was perpendicular to the axis of a graphite tube heater 6 × 5 × 12 mm. KCl/NaCl P-V-T cross-calibration experiments (*Walker et al.* [2002] in which NaCl was packed above the thermocouple with KCl below) were used to find a secondary reference equation of state (EOS) for KCl. In the $KClO_3$ and $KClO_4$ decomposition runs, except 27 April 1998, Tables 2 and 3, NaCl was packed above the thermocouple for occasional cross checks on the B2 KCl internal pressure standard. The press was moved up and down to switch the beam alternately between the NaCl and the B2 KCl or $KClO_3$. The heater axis was perpendicular to the beam, oblique to the (111) anvil truncation, and parallel to the gap between WC anvils. This geometry was achieved by spanning the gap between anvils (2 at each end) and making contact with the heater tube with a 6 × 1.5 mm stainless steel disc. Press characteristics, pressure media, and gaskets were otherwise as given by *Walker et al.* [2001] and *Johnson et al.* [2001].

3. Chloride Pressure Standards

[10] Most experiments contained at least some B2 KCl either as material originally present or produced from incipient $KClO_3$ decomposition. Copious amounts of B2 KCl appear as disproportionation and then decomposition reactions proceed. Thus B2 KCl cell volume is a suitable internal standard for determining the pressure for each EDXRD spectrum at known temperature once its EOS is known. The

Table 1. EOS Parameters

		Cell or Molar Volume			K_o		α_o	
Phase	V*, V_o	$Å^3$/cell	(Z)	cm^3/mol	kbar	K'_o	K^{-1}	
B2 KCl	V*	53.53	1	32.25	237	4.4	0.00018	*Walker et al.* [2002][a]
	*V**	*54.52*		*32.84*	*168*	*7*		*Vaidya and Kennedy* [1971][b]
	*V**	*54.39*		*32.76*	*196*	*5.3*		*Yagi* [1978][b]
	*V**	*52.85*		*31.83*	*287*	*[4]*		*Campbell and Heinz* [1991]
	*V**	*55.21*		*33.25*	*173*	*4.4*		*Hofmeister* [1997]
R $KClO_3$	V*	236.6	3	47.50	249	5.1	0.00018	
O $KClO_4$	V_o	363.84	4	54.87	207	5.9	0.00013	
O_2	V*			11.5	121	11.4	0.00018	EOS fit[c]
	*V**			*10.5*	*314*	*6.4*	*0.00017*	Point fit

V_o is the measured ambient volume. V* is the fictive volume the phase would have at ambient if stable in same form. *Italicized* multiple entries show range of parameters that produce similar fits to the data within the measured range.

[a] EOS used to determined pressure from B2 KCl spectra at known T.

[b] Parameters derived from fitting published B2 data with Birch EOS.

[c] EOS used to extrapolate oxygen volume in Figure 1B as 7.9 cm^3/mol at 2500°C, 300 kbar.

Eulerian strain, *f*, for volume V compared to ambient volume V_o

$$f = 0.5\left[(V/V_o)^{-2/3} - 1\right]$$

is used in the thermal *Birch* [1986] equation, in which $\alpha_o K_o$ is taken to be constant,

$$P = 3K_o f(1+2f)^{2.5}\left[1 + (3/2)f\left(K'_o - 4\right)\right] + \alpha_o K_o \Delta T$$

where ΔT is the difference in temperature from ambient T where V_o is taken, α_o is the zero-pressure, 298 K thermal expansion, K_o is the bulk modulus, and K'_o is the pressure derivative of the bulk modulus. Table 1 lists values of these parameters for B2 KCl determined in a separate cross-calibration study against cocompressed B1 NaCl [*Walker et al.*, 2002]. The B2 KCl EOS parameters recover the ambient-temperature compressions of *Vaidya and Kennedy* [1971] to 45 kbar and of *Yagi* [1978] to 90 kbar, and give very adequate descriptions of the much higher-pressure, ambient-temperature DAC compressions of B2 KCl reported by *Campbell and Heinz* [1991]. The values of the B2 KCl parameters are not individually an especially close match to any of those from the values of *Vaidya and Kennedy* [1971], *Yagi* [1978], *Campbell and Heinz* [1991], or *Hofmeister* [1997]. But the tradeoffs between V_o, K_o, and K'_o render them collectively in reasonable agreement as a description of the ambient B2 data arrays. Thus errors on individual parameters are not meaningful or individually quoted. Further analysis may be found in the work of *Walker et al.* [2002]. Table 1 provides, in addition, a thermal expansion value derived from simultaneously heated and compressed B2 KCl. *Birch*'s [1986] B1 NaCl EOS (form BE_2 with constant $\alpha_o K_o$ of 0.0286 kbar/K), largely determined by reprocessing *Boehler and Kennedy*'s [1980] and *Fritz et al.*'s [1971] data, was the reference EOS for determining the B2 KCl EOS. From 5 to 8 peaks were observed for NaCl, indexed, and refined to give unit cell volumes to 0.1% or better. Programs XFIT of the Koalariet package [*Cohelo and Cheary*, 1997] and UNITCELL [*Holland and Redfern*, 1997] were used for peak fitting and cell refinement. The separate NaCl spectra are simpler than the mixed K-chloride-chlorate-perchlorate spectra for which the Rietica package was useful as described below. The agreement in pressure between the separate NaCl and mixed polyphase KCl spectra listed in run Table 2 is quite satisfactory.

4. Chlorates

[11] The volume of R $KClO_3$ was tracked until its disproportionation to O $KClO_4$ and B2 KCl at about 500°C at pressures from ~20 to 90 kbar. About 6–12 peaks could be observed, indexed and refined for

Table 2. On-line In Situ XRD Results From Daresbury Station 16.4

Press load (kN)	Temperature (°C)	NaCl Pressure			B2-KCl Pressure		$KClO_3$	B2-KCl Volume		R $KClO_3$ (~Å or $Å^3$/cell)					
		Spec no.	kbar	*esd*	kbar	*esd*	Spec no.	A^3/cell	*esd*	a	*esd*	c	*esd*	vol	*esd*
2000	490				**26.2**	*0.02*	r34227	50.924	*0.003*						
2000	500				**26.4**	*0.01*	r34231	50.938	*0.003*						
2000	510				**26.6**	*0.02*	r34235	50.958	*0.003*						
2000	520				**26.4**	*0.01*	r34239	51.030	*0.003*						
2000	530				**26.2**	*0.01*	r34243	51.123	*0.003*						
2000	540				**25.5**	*0.01*	r34247	51.287	*0.002*						
2000	550				**23.4**	*0.01*	r34251	51.732	*0.002*						
2000	560				**21.5**	*0.01*	r34255	52.155	*0.003*						
2000	570				**19.0**	*0.01*	r34259	52.705	*0.002*						
2000	580				**17.0**	*0.01*	r34263	53.191	*0.002*						
2000	590				**15.5**	*0.01*	r34267	53.592	*0.003*						
2000	600				**15.2**	*0.02*	r34271	53.721	*0.004*						
2000	650				**15.2**	*0.02*	r34275	54.036	*0.004*						
2000	700				**16.5**	*0.02*	r34279	54.052	*0.004*						
2000	750				**18.6**	*0.02*	r34283	53.894	*0.004*						
2000	800				**19.6**	*0.02*	r34287	53.977	*0.004*						
2000	880				**21.2**	*0.02*	r34291	54.121	*0.004*						
2000	900				**21.6**	*0.02*	r34295	54.168	*0.004*						
2000	980				**23.8**	*0.02*	r34299	54.162	*0.004*						
2000	1000				**24.6**	*0.02*	r34307	54.123	*0.006*						
2000	1025[a]				**26.6**	*0.03*	r34315	53.815	*0.007*						
3000	20.3	r45679	**57.7**	*0.5*			r45683			5.5826	*0.0002*	7.5508	*0.0004*	203.80	*0.02*
3000	100						r45687			5.5933	*0.0002*	7.5606	*0.0004*	204.85	*0.02*
3000	150						r45691			5.6022	*0.0002*	7.5679	*0.0004*	205.70	*0.02*
3000	200	r45699	**57.9**	*0.3*			r45695			5.6110	*0.0001*	7.5777	*0.0003*	206.61	*0.01*
3000	250	r45703	**58.7**	*0.3*			r45707			5.6161	*0.0002*	7.6063	*0.0003*	207.76	*0.01*
3000	300						r45711			5.6226	*0.0002*	7.6160	*0.0003*	208.51	*0.01*
3000	350						r45715			5.6337	*0.0002*	7.6300	*0.0003*	209.72	*0.01*
3000	375						r45719			5.6435	*0.0002*	7.6428	*0.0004*	210.81	*0.02*
3000	400						r45723			5.6501	*0.0002*	7.6505	*0.0004*	211.51	*0.02*
3000	420	r45731	**54.7**	*0.2*	**53.9**	*0.05*	r45735	46.811	0.005	5.6521	*0.0002*	7.6570	*0.0005*	211.84	*0.02*
3000	440				**54.4**	*0.05*	r45739	46.823	0.006	5.6569	*0.0002*	7.6631	*0.0005*	212.37	*0.02*
3000	460				**54.1**	*0.04*	r45743	46.921	0.005	5.6625	*0.0003*	7.6664	*0.0006*	212.88	*0.02*
3000	480				**54.1**	*0.03*	r45747	46.980	0.004	5.6679	*0.0003*	7.6659	*00000*	213.28	*0.03*
3000	500				**53.2**	*0.03*	r45751	47.145	0.004	5.6758	*0.0005*	7.6607	*0.0013*	213.73	*0.04*
3000	520				**53.1**	*0.02*	r45755	47.221	0.002						
3000	540				**52.4**	*0.01*	r45759	47.368	0.002						
3000	560				**51.2**	*0.01*	r45763	47.585	0.001						
3000	580				**50.1**	*0.01*	r45767	47.788	0.001						
3000	580	r45775	**47.0**	0.1	**48.7**	*0.02*	r45771	47.960	0.002						
4000	20	r45387	**79.9**	*0.5*			r45391			5.5190	*0.0002*	7.4349	*0.0004*	196.12	*0.01*
4000	100						r45395			5.5280	*0.0002*	7.4407	*0.0005*	196.92	*0.02*
4000	150						r45399			5.5344	*0.0002*	7.4464	*0.0004*	197.53	*0.01*
4000	170						r45403			5.5360	*0.0002*	7.4483	*0.0004*	197.69	*0.01*
4000	180						r45407			5.5371	*0.0002*	7.4499	*0.0004*	197.81	*0.01*
4000	200	r45415	**80.4**	*0.5*			r45411			5.5386	*0.0002*	7.4523	*0.0005*	197.98	*0.02*
4000	220	r45419	**80.4**	*0.5*			r45423			5.5397	*0.0001*	7.4540	*0.0003*	198.10	*0.01*
4000	240						r45427			5.5408	*0.0002*	7.4577	*0.0004*	198.28	*0.01*
4000	260						r45431			5.5424	*0.0002*	7.4602	*0.0004*	198.46	*0.01*
4000	280						r45435			5.5450	*0.0002*	7.4637	*0.0003*	198.74	*0.01*
4000	300						r45439			5.5478	*0.0002*	7.4675	0.0004	199.04	*0.01*
4000	320						r45443			5.5514	*0.0002*	7.4719	*0.0004*	199.42	*0.01*
4000	340						r45447			5.5571	*0.0002*	7.4783	*0.0004*	200.00	*0.01*
4000	360						r45451			5.5647	*0.0002*	7.4869	*0.0004*	200.78	*0.01*
4000	380						r45455			5.5689	*0.0002*	7.4922	*0.0004*	201.22	*0.01*
4000	400	r45463	**74.2**	*0.3*			r45459			5.5700	*0.0003*	7.5305	*0.0003*	202.33	*0.02*
4000	420	r45467	**75.8**	*0.2*	**76.5**	*0.05*	r45471	44.565	*0.005*	5.5876	*0.0003*	7.5199	*0.0004*	203.33	*0.02*
4000	440				**76.7**	*0.04*	r45475	44.596	*0.003*	5.5865	*0.0004*	7.5162	*0.0006*	203.15	0.03

Table 2. (continued)

O $KClO_4$ (Å or $Å^3$/cell)								O_2 Fluid Volume (cm^3/mol)			
a	*esd*	b	*esd*	c	*esd*	vol	*esd*	$KClO_3$-KCl	*esd*	$KClO_4$-KCl	*esd*
8.6475	*0.0008*	5.5737	*0.0006*	7.0963	*0.0008*	342.03	*0.06*			10.43	*0.02*
8.6509	*0.0008*	5.5750	*0.0006*	7.0964	*0.0007*	342.25	*0.06*			10.44	*0.02*
8.6548	*0.0008*	5.5751	*0.0006*	7.0996	*0.0007*	342.56	*0.06*			10.46	*0.02*
8.6628	*0.0009*	5.5796	*0.0007*	7.1028	*0.0008*	343.32	*0.06*			10.49	*0.03*
8.6744	*0.0009*	5.5824	*0.0007*	7.1045	*0.0008*	344.03	*0.07*			10.52	*0.03*
8.6848	*0.0009*	5.5891	*0.0007*	7.1144	*0.0008*	345.33	*0.07*			10.57	*0.03*
8.7219	*0.0011*	5.6029	*0.0008*	7.1305	*0.0010*	348.46	*0.08*			10.67	*0.03*
8.7932	*0.0014*	5.6099	*0.0009*	7.1380	*0.0009*	352.11	*0.09*			10.82	*0.03*
8.8349	*0.0014*	5.6288	*0.0009*	7.1637	*0.0011*	356.25	*0.10*			10.96	*0.04*
8.8692	*0.0015*	5.6460	*0.0012*	7.1913	*0.0013*	360.12	*0.12*			11.11	*0.04*
								9.57	*0.02*		
8.3834	*0.0015*	5.4679	*0.0012*	6.9141	*0.0014*	316.94	*0.11*	9.63	*0.02*	9.77	*0.05*
8.3916	*0.0011*	5.4663	*0.0008*	6.9222	*0.0010*	317.53	*0.08*	9.66	*0.02*	9.79	*0.03*
8.3961	*0.0008*	5.4669	*0.0006*	6.9261	*0.0008*	317.91	*0.06*	9.69	*0.02*	9.80	*0.03*
8.4051	*0.0006*	5.4704	*0.0004*	6.9310	*0.0005*	318.68	*0.04*	9.69	*0.03*	9.81	*0.02*
8.4118	*0.0005*	5.4755	*0.0003*	6.9364	*0.0005*	319.48	*0.04*			9.84	*0.01*
8.4212	*0.0005*	5.4802	*0.0003*	6.9431	*0.0005*	320.42	*0.04*			9.87	*0.01*
8.4357	*0.0006*	5.4870	*0.0004*	6.9521	*0.0005*	321.79	*0.04*			9.91	*0.02*
8.4442	*0.0009*	5.4928	*0.0006*	6.9595	*0.0007*	322.80	*0.06*			9.92	*0.02*
8.2562	*0.0000*	5.3780	*0.0000*	6.8102	*0.0000*	302.39	*0.00*				
8.2555	*0.0011*	5.3783	*0.0009*	6.8118	*0.0010*	302.45	*0.08*	9.33	*0.02*	9.36	*0.03*
8.2550	*0.0010*	5.3777	*0.0006*	6.8124	*0.0006*	302.42	*0.06*	9.29	*0.02*	9.35	*0.02*

Table 2. (continued)

Press load (kN)	Temperature (°C)	NaCl Pressure			B2-KCl Pressure		$KClO_3$	B2-KCl Volume		R $KClO_3$ (~Å or $Å^3$/cell)					
		Spec no.	kbar	*esd*	kbar	*esd*	Spec no.	A^3/cell	*esd*	a	*esd*	c	*esd*	vol	*esd*
4000	460				**77.1**	*0.05*	r45479	44.608	*0.004*	5.5905	*0.0006*	7.5262	*0.0004*	203.71	*0.03*
4000	480				**76.2**	*0.01*	r45483	44.740	*0.001*						
4000	500	r45491	**75.1**	*0.4*	**76.0**	*0.01*	r45487	44.805	*0.001*						
4000	520	r45495	**74.9**	*0.2*	**75.9**	*0.01*	r45499	44.868	*0.001*						
4000	540				**76.1**	*0.01*	r45503	44.898	*0.001*						
4000	560				**75.7**	*0.01*	r45507	44.981	*0.001*						
4000	580				**75.7**	*0.01*	r45511	45.040	*0.001*						
4000	600	r45519	**74.5**	*0.8*	**75.7**	*0.02*	r45515	45.090	*0.002*						
							(*possibly not R KClO3*)								
5000	20	r45547	**93.6**	*0.9*			r45551			5.4629	*0.0002*	7.3590	*0.0011*	190.20	*0.03*
5000	100						r45555			5.4737	*0.0001*	7.3610	*0.0006*	191.00	*0.02*
5000	150						r45559			5.4793	*0.0002*	7.3646	*0.0011*	191.48	*0.03*
5000	200	r45567	**94.3**	*0.8*			r45563			5.4846	*0.0002*	7.3677	*0.0011*	191.93	*0.03*
5000	250	r45571	**94.4**	*0.7*			r45575			5.4911	*0.0002*	7.3694	*0.0011*	192.43	*0.03*
5000	300						r45579			5.4966	*0.0002*	7.3742	*0.0011*	192.95	*0.03*
5000	350						r45583			5.5047	*0.0002*	7.3860	*0.0011*	193.83	*0.03*
5000	400	r45591	**93.6**	*0.4*			r45587			5.5145	*0.0002*	7.3927	*0.0011*	194.69	*0.03*
5000	420	r45595	**94.1**	*0.4*	**90.0**	*0.05*	r45599	43.440	*0.004*	5.5143	*0.0002*	7.3799	*0.0007*	194.34	*0.02*
5000	440				**90.1**	*0.04*	r45603	43.471	*0.003*	5.5149	*0.0002*	7.3774	*0.0007*	194.32	*0.02*
5000	460				**90.2**	*0.04*	r45607	43.513	*0.003*	5.5203	*0.0003*	7.3844	*0.0009*	194.88	*0.03*
5000	480				**90.0**	*0.03*	r45611	43.568	*0.002*	5.5276	*0.0003*	7.3967	*0.0008*	195.72	*0.02*
5000	500	r45619	**89.6**	*0.2*	**90.1**	*0.03*	r45615	43.603	*0.002*	5.5339	*0.0003*	7.4101	*0.0009*	196.53	*0.03*
5000	520	r45623	**89.8**	*0.2*	**90.6**	*0.02*	r45627	43.609	*0.002*						
5000	540				**90.8**	*0.02*	r45631	43.641	*0.002*						
5000	560				**91.6**	*0.02*	r45635	43.621	*0.002*						
5000	580				**91.2**	*0.02*	r45639	43.694	*0.002*						
5000	600				**91.8**	*0.01*	r45643	43.692	*0.001*						
5000	620	r45651	**90.3**	*0.2*	**91.8**	*0.02*	r45647	43.740	*0.002*						

[a] Data collection on B2-KCl until just before melting.

R $KClO_3$, whereas about 15 could usually be tracked for O $KClO_4$. The Rietica for MS Windows Rietveld program [*Hunter*, 1998] was used in Lebail mode [*Le Bail et al.*, 1988]. Structureless, "whole profile" fits were performed to the overlapping, multiphase powder diffraction patterns of R $KClO_3$, O $KClO_4$, and B2 KCl. The primary inputs for the Le Bail method are approximate starting unit-cell values and accurate space group information. The raw energy-dispersive channel data was converted into a 2-theta, angular dispersive scale suitable for Le Bail analysis with Rietica using the DLConvert 1.26 for MS Windows software provided by the Daresbury 16.4 Beamline [*Smith and Gontier*, 1999]. Within Rietica, a Pseudo-Voight profile function was applied, an Automatic Smoothed function was used for background fitting; and width and shape functions were varied to provide the best whole profile visual fit to the diffraction data. The unit-cell constants refined by Rietica gave phase volumes to better than 0.1% uncertainty. These measurements have been compiled in Table 2 and Figures 4 and 5 and fit to thermal Birch EOS. $KClO_4$ has been tracked over the limited temperature interval in which it is stable in a $KClO_3$ + KCl bulk composition, roughly from 400°C to 600°C at pressures from 20 to 90 kbar. Consequently $KClO_4$ thermal expansion is less well constrained because its absence below 400°C and complete decomposition above 600°C truncates the temperature range over which we can observe its expansion.

[12] Phase volumes for B2 KCl, R $KClO_3$ and O $KClO_4$ are recorded in Table 2 as a function of *P* and T. The refined values of R $KClO_3$ cell volume from the present data set and that of

Table 2. (continued)

O $KClO_4$ (Å or $Å^3$/cell)								O_2 Fluid Volume (cm^3/mol)			
a	*esd*	b	*esd*	c	*esd*	vol	*esd*	$KClO_3$-KCl	*esd*	$KClO_4$-KCl	*esd*
8.2575	*0.0008*	5.3830	*0.0006*	6.8152	*0.0006*	302.94	*0.05*	9.36	*0.02*	9.38	*0.03*
8.2634	*0.0008*	5.3873	*0.0006*	6.8224	*0.0006*	303.71	*0.05*			9.40	*0.02*
8.2661	*0.0008*	5.3919	*0.0006*	6.8257	*0.0006*	304.22	*0.05*			9.42	*0.02*
8.2664	*0.0013*	5.3932	*0.0010*	6.8281	*0.0009*	304.41	*0.08*			9.42	*0.03*
8.2642	*0.0016*	5.3969	*0.0011*	6.8298	*0.0011*	304.61	*0.10*			9.42	*0.03*
(*possibly not R KClO3*)											
8.1807	*0.0018*	5.3414	*0.0016*	6.7546	*0.0015*	295.15	*0.13*			9.15	*0.05*
8.1818	*0.0015*	5.3400	*0.0012*	6.7617	*0.0011*	295.42	*0.10*			9.16	*0.04*
8.1851	*0.0016*	5.3438	*0.0012*	6.7592	*0.0011*	295.65	*0.10*			9.17	*0.04*
8.1938	*0.0010*	5.3411	*0.0006*	6.7632	*0.0007*	295.98	*0.06*			9.17	*0.02*
8.1917	*0.0009*	5.3441	*0.0005*	6.7641	*0.0006*	296.11	*0.05*			9.17	*0.02*
8.1981	*0.0006*	5.3462	*0.0003*	6.7688	*0.0005*	296.67	*0.04*			9.21	*0.02*
8.1979	*0.0007*	5.3507	*0.0003*	6.7694	*0.0005*	296.94	*0.04*			9.22	*0.02*
8.1985	*0.0006*	5.3535	*0.0003*	6.7710	*0.0005*	297.18	*0.03*			9.25	*0.01*
8.2007	*0.0009*	5.3562	*0.0004*	6.7736	*0.0008*	297.53	*0.05*			9.25	*0.02*
8.2003	*0.0011*	5.3601	*0.0006*	6.7787	*0.0012*	297.95	*0.07*			9.29	*0.03*

Johnson et al. [2001] are both shown in Figure 4. Our highest pressure $KClO_3$ decomposition, near 90 kbar, produces $KClO_3$ volumes that are anomalously lower than extrapolations of the data from less than 80 kbar. We suspect that a subtle phase transition within $KClO_3$ may be responsible for this anomaly (although other evidence in the form of peak splittings or extinctions is difficult to recognize in the presence of O $KClO_4$ and B2 KCl). The fact that the deviations are to lower volumes is consistent with a phase change encountered with increasing pressure. We exclude the ∼90 kbar data set from our R $KClO_3$ fitting. The V_o of 236.6 $Å^3$/cell (Z = 3) is our extrapolation of the metastable volume that R $KClO_3$ would have if it were recoverable at ambient conditions. It is not quenchable and is simply a reference volume to parameterize the EOS information. In contrast, in fitting the O $KClO_4$ data, V_o at ambient is measured to be 363.8 A^3/cell (Z = 4). O $KClO_4$ is stable from ambient to at least 90 kbar at temperatures up to its decomposition. Thus V_o provides a valuable constraint on the O $KClO_4$ EOS. The $KClO_4$ data encountered in the data collected for R $KClO_3$ by *Johnson et al.* [2001] are also shown in Figure 5. Both data sets are completely conformable and are fit together.

[13] For $KClO_3$ bulk compositions, O $KClO_4$ is produced by the incongruent disproportionation of R $KClO_3$ to O $KClO_4$ and B2 KCl. We subsequently observe the product O $KClO_4$ to decompose to B2 KCl plus inferred fluid O_2. $KClO_3$ was used as the reactant for examining the oxygen-producing equilibria for several reasons. First was to check our earlier results on $KClO_3$ [*Johnson et al.*, 2001] with new detector, calibration, illumination, and data reduction procedures. Second, use of $KClO_3$ also

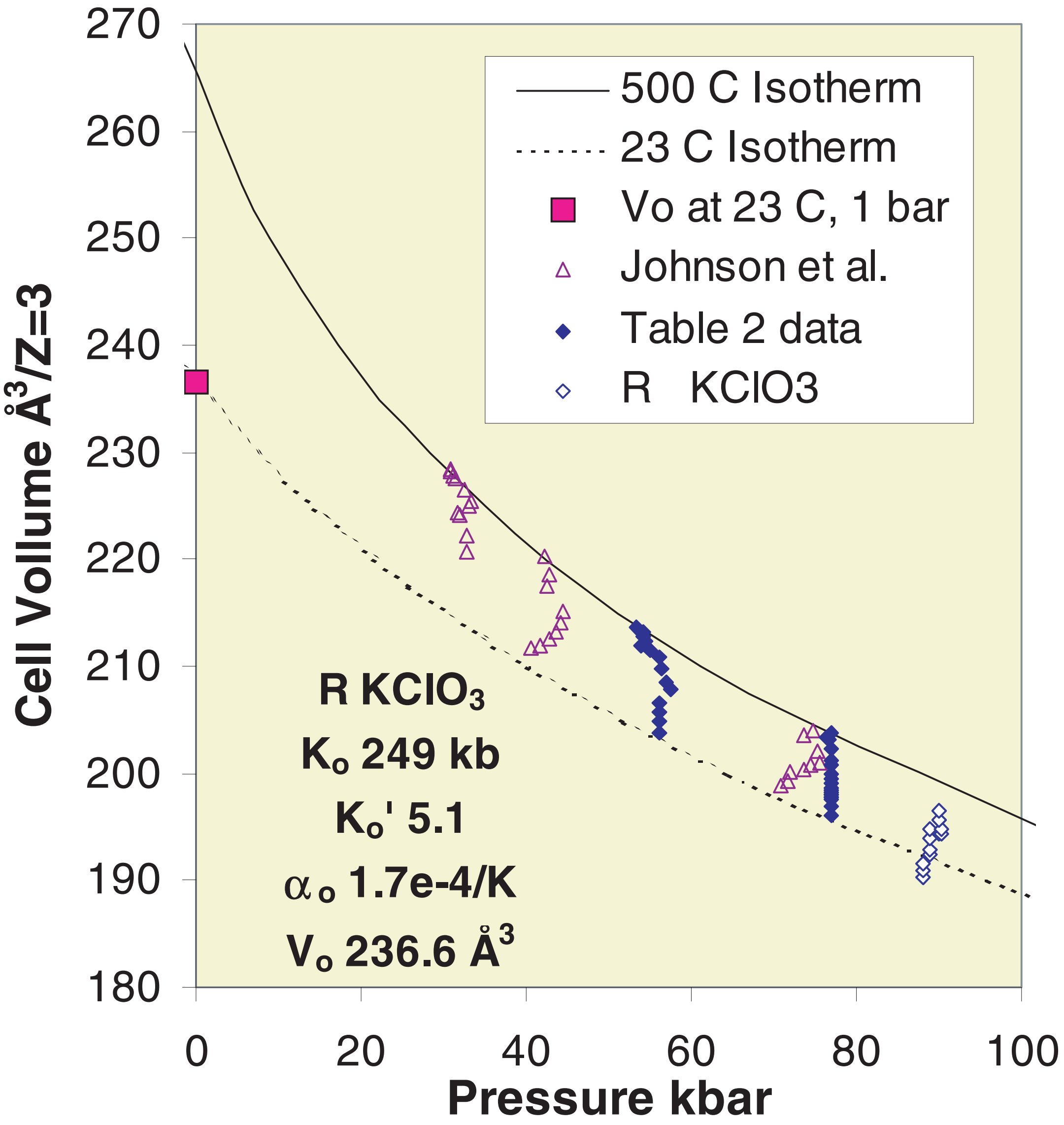

Figure 4. Unit cell volume of $KClO_3$ as a function of pressure from Table 2. EOS parameters of the Birch form recovered by fitting all data except the 90 kbar information, which may no longer be rhombohedral (R? $KClO_3$). Isotherms are computed from the Birch EOS parameters. Agreement between the 1997 data set reported by *Johnson et al.* [2001] and the 1998 data reported here in Table 2 is acceptable. The V_o parameter must be recovered from fitting because R $KClO_3$ does not quench from the P-T range of its stability to be able to be measured at ambient.

allows the $KClO_4$ decomposition equilibrium to be examined with the loading of a single substance because $KClO_3$ disproportionates to $KClO_4$ before O_2-liberating decomposition occurs. This dual experiment strategy cannot be followed using $KClO_4$ as the bulk composition unless one performs experiments at higher pressure than the four-phase invariant point R $KClO_3$ + O $KClO_4$ + B2 KCl + fluid O_2. From our Schreinemakers analysis presented below it appears that this invariant point is at pressures above those we were able to investigate. And third, the presence of a small excess of KCl in the $KClO_3$ insures that the $KClO_3$ and $KClO_4$ compositions in the experiments are buffered against having excess O_2. Although we have no evidence for any such phase nonstoichiometry (and have some evidence against in the stoichiometric decomposition weights of $KClO_4$), the precaution of buffering

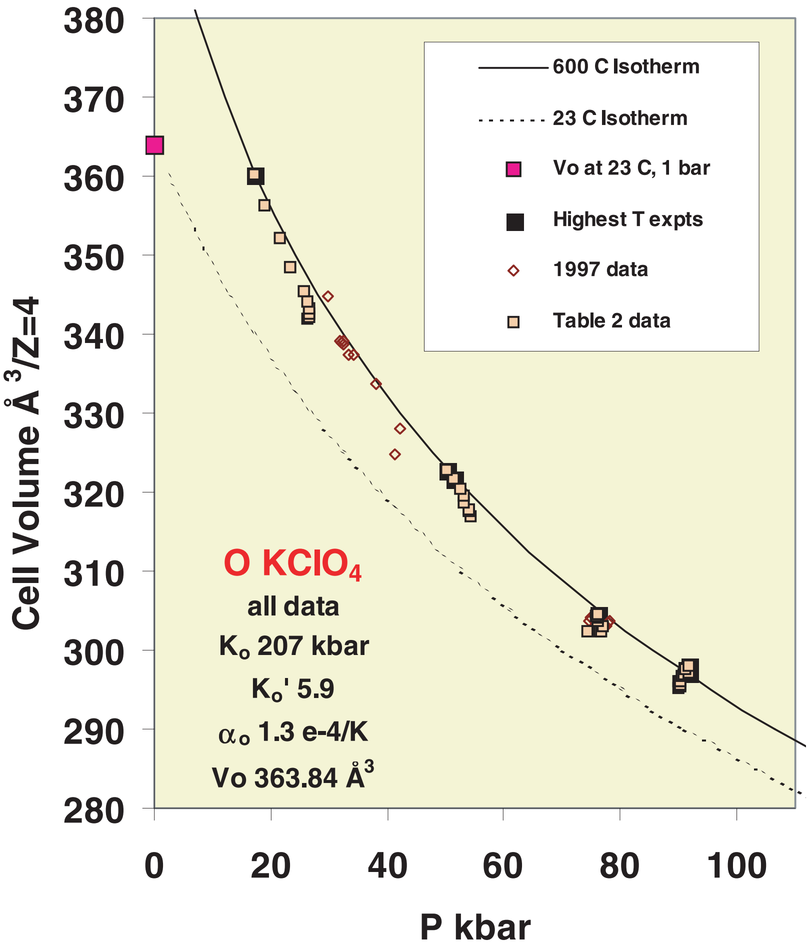

Figure 5. Unit cell volume of O $KClO_4$ as a function of pressure from Table 2. O $KClO_4$ is stable from ambient to the highest pressures studied, so V_o is known by direct measurement to be 363.8 Å^3/cell (Z = 4) and provides a constraint on the fitting rather than being another variable to be fit. 1997 data for R $KClO_4$ (not reported by Johnson et al.) and 1998 data of Table 2 in this study are consistent and fit together. Isotherms computed from the Birch EOS parameters recovered in this fitting.

the phase compositions by using starting $KClO_3$ with a small excess of KCl is prudent and painless.

5. Phase Stability

[14] Table 3 contains the temperature, pressure, duration, and phases observed in experiments run on-line at Daresbury's Station 16.4 and off-line at LDEO and DL. The four on-line temperature sequences at constant press forces of 2000–5000 kN all show by XRD that R-$KClO_3$ disproportionates with increasing temperature to O $KClO_4$ and B2 KCl which assemblage in turn decomposes to only B2 KCl as an X-ray-scattering phase at the highest temperatures. We interpret these in situ XRD observations in terms of the following sequence of reactions in KCl-O_2 occurring with increasing temperature:

$$4\ \text{R-KClO}_3 = 3\ \text{O-KClO}_4 + \text{B2-KCl} \qquad (2)$$

followed by:

$$\text{O-KClO}_4 = \text{B2-KCl} + 2\ \text{O}_2 \qquad (3)$$

Johnson et al. [2001] presented a Schreinemakers analysis of this system and concluded that

$$\text{R-KClO}_3 = \text{B2-KCl} + 3/2\ \text{O}_2 \qquad (4)$$

should be metastable with respect to (2) and (3) in the pressure range of the experiments and should occur metastably between them in temperature.

Table 3. Experimental Results

On-line phase observations, $KClO_3$ in graphite heater, Station 16.4, Daresbury Lab

	$KClO_3$		$KClO_4$		P range, kbar	
	Low T	Top T	Low T	Top T	Low T[a]	Top T[a]
27 April 1998	[b]	[b]	490[b]	580	26	17
11 September 1998	23	500	440	580	54	48
7 September 1998	23	460	400	520	77	76
9 September 1998	23	500	420	600	92	90

Off-line, sealed Au tubes, L-DEO and DL, $KClO_3$ bulk composition

		°C		min			
	P (kbar)	Initial	Final	Initial	Final	Reactants	Products (solids recognized by optics)
TT-392	30	500		30		$KClO_3$	$KClO_3$
TT-391	30	525		26		$KClO_3$	$KClO_4$ + KCl[c]
TT-390	30	550		20		$KClO_3$	KCl (+ quench trace $KClO_3$)
TT-385	30	575		10		$KClO_3$	KCl (+ quench trace $KClO_3$)
GG-783	30	525	560	34	15	$KClO_4$ + KCl[c]	$KClO_4$ + KCl
GG-784	30	525	579	30	30	$KClO_4$ + KCl[c]	KCl (+ quench trace $KClO_3$)
TT-393	30	550	500	20	60	KCl + O_2	KCl + ∼2% $KClO_3$ (+ tr $KClO_4$)
TT-398	30	550	to 525	10°C/hr		KCl + O_2	KCl + ∼2% $KClO_3$
TT-397	30	620	to 250	20°C/hr[a]		KCl + O_2	$KClO_4$ + KC
DL-1	45	400		15		$KClO_3$	$KClO_3 \gg$ KCl (unsealed)
DL-2	45	400		2340		$KClO_3$	KCl > $KClO_3$ (unsealed)[d]
DL-3	45	400		2700		$KClO_3$	KCl > $KClO_3$ (sealed)[d]
GG-673[c]	50	550		16		$KClO_3$	$KClO_3$ (partial decomposition)
GG-674[c]	50	560		15		$KClO_3$	$KClO_4$ + KCl (no $KClO_3$)[c]
GG-681[c]	50	560	500	23	30	$KClO_4$ + KCl[c]	KCl + ∼2% $KClO_3$
TT-371[c]	58	585		10		$KClO_3$	KCl

Off-line, 1 atm of air, L-DEO, $KClO_4$ bulk composition

	°C	min	Reactant	Product
AK-1	500	85	$KClO_4$	$KClO_4$
AK-3	525	20	$KClO_4$	$KClO_4$
AK-4	530	25	$KClO_4$	$KClO_4$ + melt
AK-5	530	158	$KClO_4$	KCl + O_2 via liquid
AK-2	535	55	$KClO_4$	KCl + O_2 via liquid
AK-6	500	1205	$KClO_4$	KCl + O_2 without liquid (weight loss 46.8%)

[a] 1 atm. $KClO_4$ metastable with respect to KCl + O_2; decomposition slower at 500 than at 535°C.
[b] Data collection began in error only at 490°C and above after $KClO_3$ had disproportionated.
[c] Reported by *Johnson et al.* [2001].
[d] No $KClO_4$ in product by optics, confirmed by XRD.

Johnson et al. tracked metastable equilibrium (4) and derived oxygen volumes from it. They predicted the existence of a four-phase invariant point between B2 KCl, O $KClO_4$, R $KClO_3$, and fluid O_2 at pressures higher than those studied. Equilibrium (4) should be stable at pressures above the invariant point. They also predicted that equilibrium

$$\text{O-KClO}_4 = \text{R-KClO}_3 + 1/2\ \text{O}_2 \qquad (5)$$

would be stable above the invariant point at lower temperature than (4).

[15] Figure 6 shows a portion of the P-T net relevant to the experimental work of this study and the work of *Johnson et al.* [2001]. Reactions (2), (3), (4), and (5) are in pink, blue, red and black, respectively. The red, dashed metastable end of (4) is shown below the invariant point that is conjec-

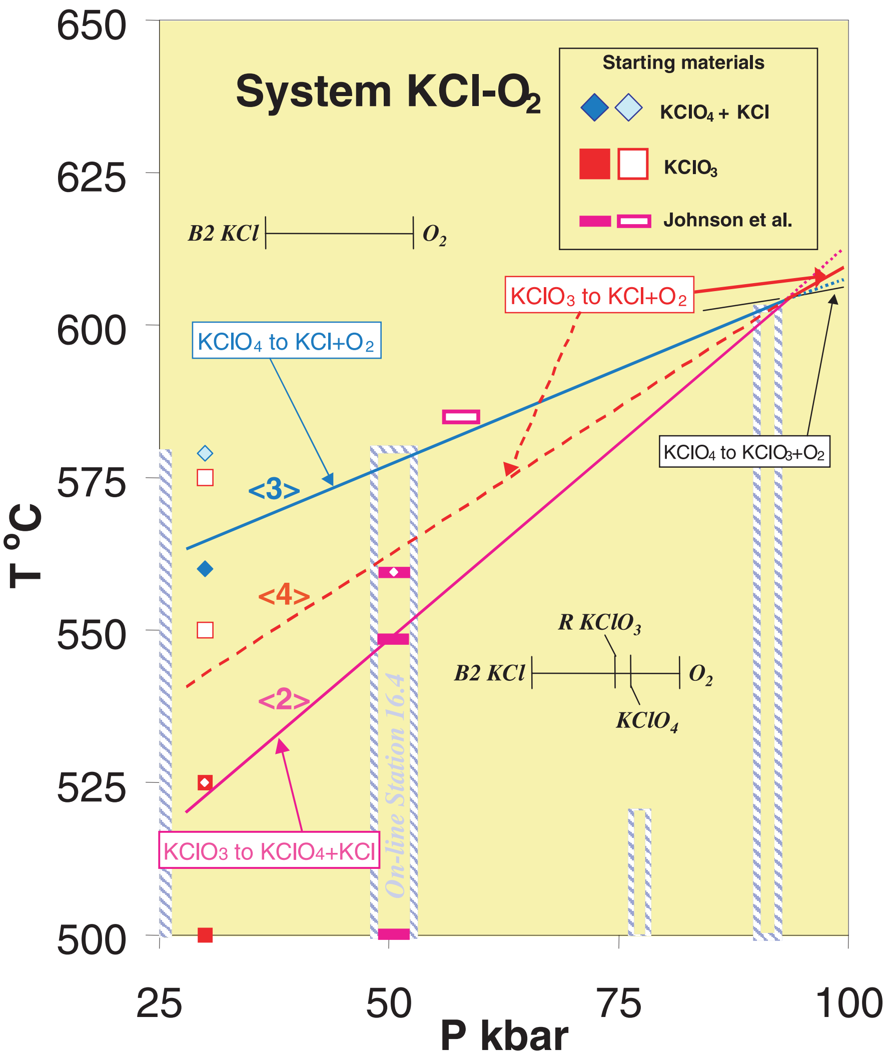

Figure 6. P-T net for KCl-O_2 system based on experiments in Table 3. Diamond outline symbols indicate runs that had $KClO_4$ + KCl (produced by $KClO_3$ disproportionation) as the starting material. Square or rectangular outline symbols indicate runs that had $KClO_3$ as the starting material. Open center symbols indicate runs that produced the assemblage KCl + O_2. Symbols with interior small white diamonds produced $KClO_4$ + KCl assemblages. The open square at 30 kbar/550°C indicates a run that decomposed to KCl + O_2 from $KClO_3$ presumably across metastable reaction (4). By contrast, the run at 30 kbar/560°C remained in the $KClO_4$ + KCl field between stable reactions (2) and (3) because it had been prereacted to form an initial starting assemblage of $KClO_4$ + KCl on the high-T side of (2).

turally shown near 100 kbar and 600°C. The equilibrium lines are drawn to be consistent with the off-line experimental data points in Table 3 and those of Johnson et al. shown for $P > 30$ kbar. Filled rectangles are for solid assemblages and open symbols for KCl + O_2 assemblages. Off-line experiments in 12 mm TEL multianvil assemblies are slightly modified from those of Johnson et al. in thermocouple placement but are the same as those of *Walker et al.* [2001] used for the study of T RbClO$_4$ decomposition. The results here are generally compatible with those of Johnson et al. at 30 kbar but there are differences in detail that may be attributed to the different thermocouple placement strategies used in the two studies.

[16] The off-line experimental data points were used to locate the equilibria because the temperatures of the on-line observations can be compromised by two factors. The $KClO_3$ in on-line

experiments is not in a sealed, inert container. R $KClO_3$ is directly against the graphite heater and any leakage of product O_2 through microcracks or any reaction with graphite to produce CO/CO_2 mixtures with O_2 will drive (3) and (4) to temperatures below the equilibrium in the KCl-O_2 system. In this context the blue striped vertical bands record the temperature range at 4 press forces on-line over which O $KClO_4$ observations could be made. These bands should be bounded by equilibria (2) and (3). Several interesting features are revealed by comparing the limits of these blue striped bands with the equilibria. First, the upper limit of the striped boxes is a fairly good approximation of the blue reaction (3) terminating O $KClO_4$ stability. The equilibria established off-line were in sealed Au tubes which are not vulnerable to gas leaks or carbon contaminations. (Au tubes could not be used on-line because of their X-ray opacity.) Thus the near correspondence of the tops of the striped boxes and the blue equilibrium (3) indicates that the on-line experiments were fairly nonporous. Second, the 4000 kN on-line experiment is a conspicuous exception with O $KClO_4$ disappearing above 520°C instead of remaining observable to ~590°C. Perhaps the experiment leaked. Third, the lower ends of the striped boxes for the on-line appearance of O $KClO_4$ are uniformly way below the reaction (2) boundary suggested from off-line experiments. Because (2) does not involve the O_2 fluid phase, its temperature is not lowered by leakage or contamination as are (3) and (4). This raises a question as to how well pink reaction (2) is located by the off-line experiments. The experiments of *Johnson et al.* [2001] above 30 kbar, reported again in Table 3, demonstrate that pink reaction (2) must be below an experiment at 560°C and 50 kbar (GG-674) because this experiment records the forward conversion of R $KClO_3$ into O $KClO_4$ and B2 KCl. The demonstration of solid-state reversal of (2) is incomplete because experiment GG-681 shows only partial conversion of O $KClO_4$ + B2 KCl back into ~2% R $KClO_3$ at 500°C. The fact that any $KClO_3$ regrows from an initially $KClO_3$-free assemblage should indicate that the final temperature is below metastable curve (4). Curve (4) is an absolute upper limit to R $KClO_3$ thermal stability and regrowth should never occur above this curve. It is somewhat dissatisfying that $KClO_3$ regrowth is so incomplete below this curve and also below (2). Presumably growth kinetics of R $KClO_3$ below (4) or (2) are much slower than decomposition kinetics which are complete in minutes above (2) or (4). In any case, the partial reversal of (2) by Johnson et al. suggests that (2) cannot be too badly mislocated, and that the considerably lower temperature appearance of $KClO_4$ in $KClO_3$ bulk compositions on-line is mysterious.

[17] This apparently greater thermal stability of O $KClO_4$ (or greater instability of $KClO_3$) on-line compared to off-line is not well understood. It is possible that the equilibria like (2) investigated by quenching off-line in Table 3 are giving a faithful account of the short-term equilibrium stabilities of the phases at timescales of at most 1/2 hour. The on-line heating sequences have durations of several hours and may be appropriate to longer-term equilibria. This does not discount the equilibrium nature of the short-term equilibria, it simply renders them metastable with respect to longer-term equilibria. We return to this theme below in a discussion of the 1 atm experiments and of a time series of DL experiments reported in Table 3.

[18] The regrowth of R $KClO_3$ achieved from the B2 KCl + O_2 assemblage by this study is likewise only partially complete. We have observed at most perhaps 2% of R $KClO_3$ regrowth from the B2 KCl + O_2 or from the $KClO_4$ + KCl assemblage upon cooling to temperatures below the metastable end of (4). The failure to achieve the complete regrowth of R $KClO_3$ from B2 KCl and O $KClO_4$ is of little consequence. The principal goal of *Johnson et al.* [2001] was to demonstrate that (4), not (2), was reversible even though metastable, and that (4) was therefore an equilibrium for oxygen volume calculation to which the Clausius−Clapeyron equation applies. We confirm that metastable reaction (4) is reversible and therefore is an equilibrium. Experiments TT-390 and TT-385 show the forward reaction and TT-393 and TT-398 demonstrate the partial back conversion. A fairly coarse cluster of R (now monoclinic on quench) $KClO_3$ is seen in a

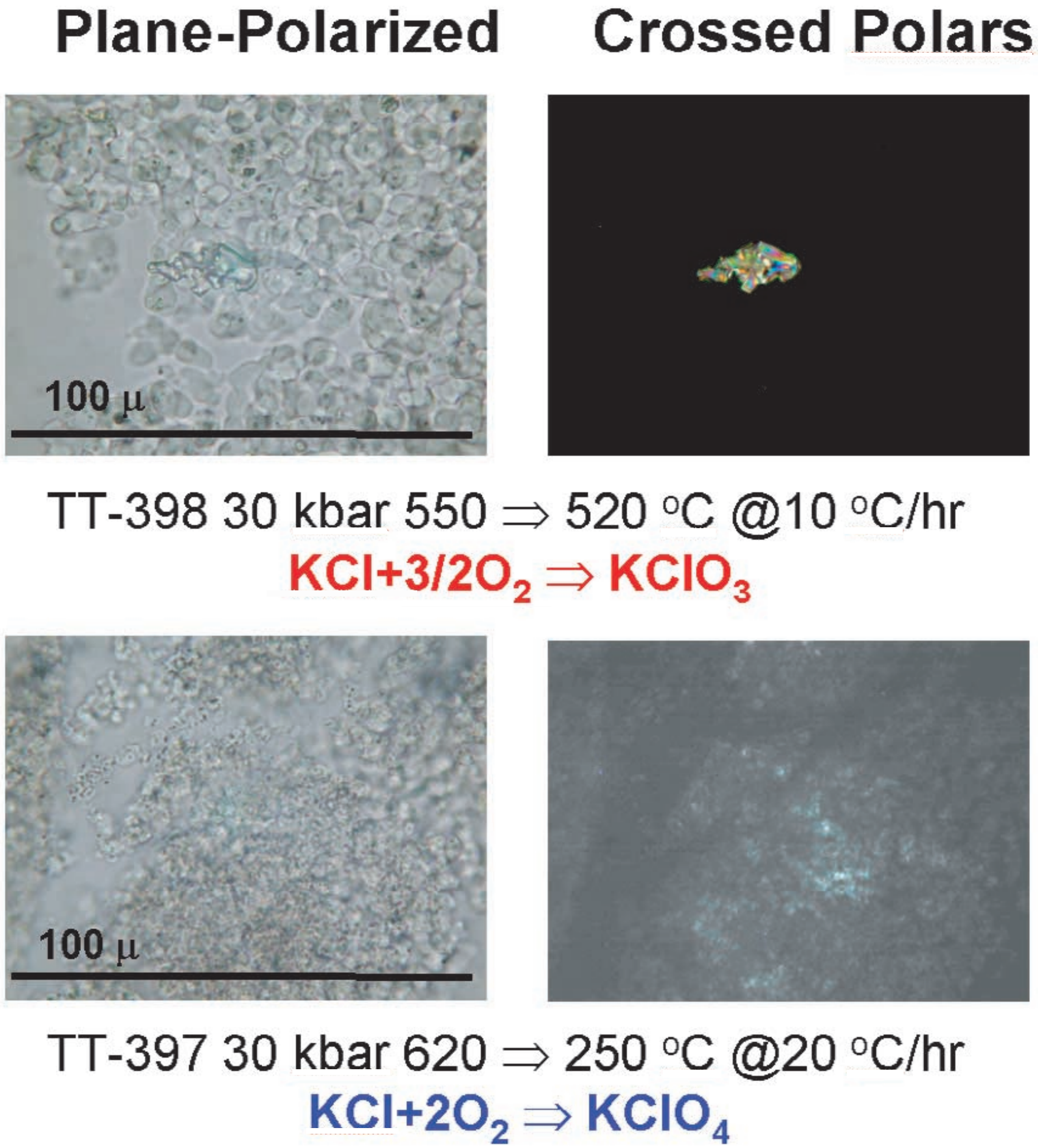

Figure 7. Photomicrographs of experimental run products in n = 1.48 refractive index oil under plane- and cross-polarized light. The *upper pair of panels* illustrates the partial reversals seen when an attempt is made to regrow $KClO_3$ by lowering T back into its field of stability. The distinctive extreme birefringence of M(onoclinic) $KClO_3$ is seen under crossed polars. The reversal is far from complete as much granular isotropic B1 KCl is also present. (M and B1 phases are observed at ambient whereas we infer from in situ XRD that R and B2 phases were present at experimental P-T.) The *lower pair of panels* illustrates the near complete reversal achieved of regrowth of $KClO_4$ + KCl from a KCl + O_2 assemblage of $KClO_3$ bulk composition. The very low birefringence of O $KClO_4$ has been digitally enhanced to make it printable. The low birefringence is visually recognizable when O $KClO_4$ is the only anisotropic phase present. In the presence of much $KClO_3$, XRD is needed to confirm the absence (or the presence) of O $KClO_4$.

field of disaggregated B2 (now B1 on quench) KCl crystals in the upper half of Figure 7. This mode of occurrence is typical of our experiments that have partially regrown $KClO_3$. (The traces of $KClO_3$ in TT-390 and TT-385 are interpreted as quench artifacts of stable KCl + O_2 assemblages because they are present as crystals an order of magnitude smaller in size and abundance without textural complexity.)

[19] Of more importance to the present study exploring the use of (3) to calculate O_2 volumes is the demonstration of reversibility of the disappearance and regrowth of O $KClO_4$. Figure 7 (lower half) shows the product of TT-397 in which an initial processing at 30 kbar and 620°C should have produced an initial B2 KCl + O_2 assemblage. Ramping this charge down at 20°C/hr to 250°C succeeded in producing copious O $KClO_4$ and B2 KCl. Although this experiment (lower half Figure 7) is very permissive with regard to the location of (3), (any temperature between 620°C and 250°C potentially qualifies) it is important in demonstrating that O $KClO_4$ can be regrown from the B2 KCl + O_2 assemblage and that (3) therefore is a reversible equilibrium.

[20] The P-T net construction of Figure 6 requires that the B2 KCl + O_2 assemblage is achieved at lower temperature from R $KClO_3$ starting material than from O $KClO_4$-bearing assemblage. [The red, dashed line is below the blue line.] Indeed experiment TT-390 at 30 kbar renders $KClO_3$ to B2 KCl + O_2 in 20 min. By contrast experiment GG-783 shows that the O $KClO_4$ + KCl assemblage persists for at least 15 min at a higher temperature, 560°C, without decomposing to B2 KCl + O_2. This difference in the persistence of the assemblages $KClO_3$ versus $KClO_4$ + KCl before decomposing to KCl + O_2 is as expected from the P-T net construction of Figure 6.

[21] In considering the stability of the various assemblages, thermochemical information would be a valuable supplement. Of the chlorates we have studied, O $KClO_4$, M $KClO_3$, R $KClO_3$, O $RbClO_4$, and T $RbClO_4$, thermochemical information is only known for O $KClO_4$ [*Chase*, 1998]. At 1 atm, O $KClO_4$ is unstable with respect to B1 KCl + O_2 by 108 kJ/mol at 298 K, the instability growing with temperature. It is interesting to compare our experimental results with this baseline. At 500°C $KClO_4$ is persistent on the timescale of an hour (AK-1). However, on the timescale of a day (AK-6), it fully decomposes to KCl + O_2 as expected from thermochemistry.

[22] At 530°C, instead of decomposing directly to KCl + O_2, $KClO_4$ proceeds to decompose via the mediation of a melt phase. A fluid is not directly observed but is inferred from the meniscus-like shape the charge assumes in the crucible instead of being the usual pile of crystals. Further textural evidence of a fluid includes the presence of vesicle-like cavities in the fluid-shaped charge which presumably are the textural fossils of evolving O_2. Fluid is not observed because it crystallizes too rapidly upon charge extraction to allow direct detection. This phenomenon of melting at 1 atm *en route* to the expected decomposition is also illustrated by M $KClO_3$ and O $RbClO_4$. In these substances the crystallization kinetics from the melt are slow enough that a thin clear fluid is easily observed upon experiment extraction from the furnace and crystallization can be observed directly as the charge cools over a few tens of seconds. *Walker et al.* [2001] reported a reversible 1 atm melting of $RbClO_4$ in the presence of the expected decomposition to RbCl + O_2 gas on timescales of an hour. The melting of M $KClO_3$ is reversible at 1 atm and shows virtually no decomposition to KCl + O_2 on timescales of an hour. Collectively these 1 atm reversible chlorate melting equilibria are all metastable with respect to their chlorides and O_2 gas. But the melting equilibria can have P-T slopes, well-defined physical properties, and do have Clausius–Clapeyron equations relating them to one another.

[23] Although all the chlorates would appear to be metastable at 1 atm, they should be stabilized with pressure. Crude calculation for $KClO_4$ thermochemistry suggests that a stability relative to KCl + O_2 should be encountered between 10 and 100 kbar. To improve the calculation, the B2 KCl entropy is needed, possibly extractable from the data of *Hofmeister* [1997], and the EOS of O_2 to

these pressures must be known. But oxygen's EOS is the central point of contention surrounding this endeavor. So it is somewhat circular to assume an O_2 EOS for a calculation to demonstrate phase stability so that the Clausius–Clapeyron equation can be used to calculate O_2 volume and retrieve the O_2 EOS. At best one could try to rationalize the phase equilibria, constrained by reversals, with expected phase stability from thermochemistry. Some O_2 volumes may work and some may not work to effect the rationalization. If one further allows the possibility that the equilibria are timescale dependent, the rationalization exercise may not successfully close the thermochemistry/O_2 volume/short-term phase equilibrium gap satisfactorily. This does not obviate the connection between short term phase equilibrium and O_2 volume.

[24] Further indication of the possible presence of short-term/long-term phase equilibrium disparities may be found in the entries for DL-1 through DL-3 in Table 3. It appears that $KClO_3$ decomposes to $KCl + O_2$ at 400°C/45 kbar on the timescale of days without a $KClO_4$ intermediary even though the short term equilibrium (4) is reversible and metastable with respect to $KClO_4$-bearing equilibria in Figure 6. This is analogous to chlorate decomposition at 1 atm being mediated by reversible melting on the short-term with the melting being metastable on the long-term. Short-term equilibria are still equilibria whether or not they are metastable!

6. O_2 Volumes

[25] Figure 8a shows O_2 volumes computed from EDXRD spectra of coexisting B2 KCl and O $KClO_4$ along reaction (3) up to 600 °C. O_2 volume is also computed for reaction (3) at the 400 and 600 °C isotherms from the EOS values in Figure 5 and Table 1. The isotherms are not a fit to the data points shown but to the whole EOS for both phases. The excellent agreement between the data points for reaction (3) and the isotherms computed from EOS fits to the whole data sets for B2 KCl and O $KClO_4$ confirms that the fit through all temperatures is compatible with the observations made at the highest temperatures. The data points for (3) collected in 1997 but not reported by *Johnson et al.* [2001] are also shown in Figure 8b with the isotherms from Figure 8a. Also shown in Figure 8B are the data points reported by *Johnson et al.* [2001] for metastable reaction (4) at about 550 °C collected in 1997. The R $KClO_3$ data for (4) from the present data set collected in 1998 are also used to compute additional O_2 volumes shown in Figure 8b. The results of $RbClO_4$ decomposition [*Walker et al.*, 2001] give yet another independent measure of O_2 volume shown in Figure 8b. The agreement between these 5 data sets is encouraging. By contrast, all chlorate-based O_2 volumes are ~4 cm^3/mol lower at 100 kbar than the volumes on which Figure 1a is based. We confirm our earlier results even though those earlier results tracked a different reaction with a different detector, less secure calibration, and poorer illumination procedures. These chlorate-based values are extrapolated to 300 kbar, 2500 °C using the EOS parameters given in Figure 8a. When these new values are plotted in Figure 1b, the difficulties previously noted with reaction (1) disappear.

7. Discussion of Discrepancies

[26] Our new oxygen volume measurements show it is possible for reaction (1) to proceed forward with increasing pressure above 300 kbar because ΔV_R for Figure 1b is no longer positive at 300 kbar and 2500 °C. The compressibility of liquid is expected to be greater than solid FeO, so at $P >$ 300 kbar the new volumes of O_2 liquid are expected to cause to ${}^{L}\overline{V}_{Wüs}$ become less than ${}^{Wüs}\overline{V}$. When ${}^{L}\overline{V}_{Wüs} < {}^{Wüs}\overline{V}$ the DAC results of *Knittle and Jeanloz* [1989a, 1991] and *Goarant et al.* [1992] become plausible. The solubility of substantial FeO in liquid metal above 300 kbar implied by the DAC results is consistent with the new chlorate-decomposition-based measurements of oxygen volume, but not with the oxygen volumes of Figure 1a. The new volume results predict a balance point for reaction (1) in astonishing proximity to the P-T where it is reported to balance experimentally by Knittle and Jeanloz. The astonishment is that so simple an approximation as Figure 1 yields this result.

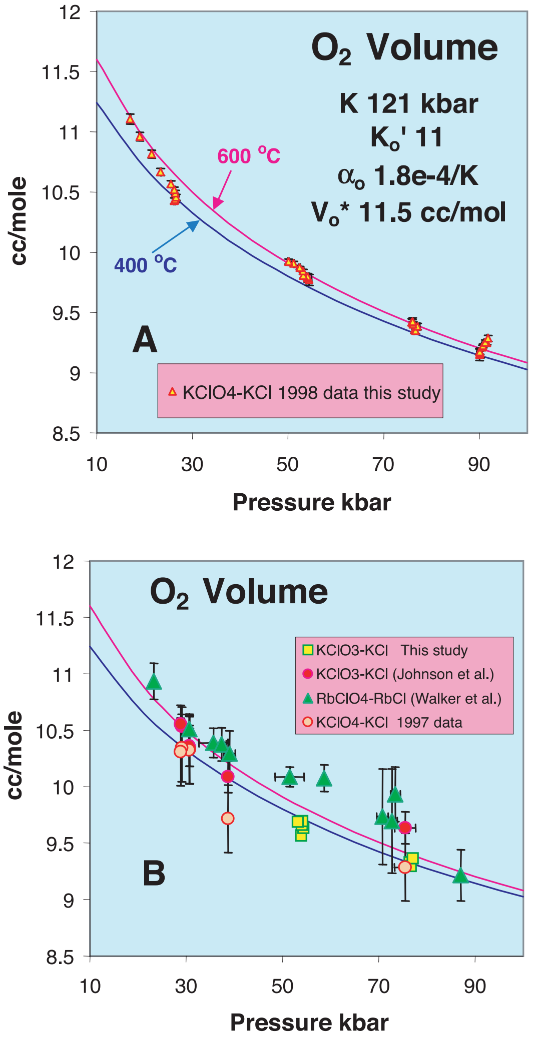

Figure 8. Oxygen volumes as a function of pressure. Part (a) computed from O $KClO_4$-B2 KCl (3). The two isotherms bound the data collection temperatures. These isotherms are computed by taking the full EOS parameters for O $KClO_4$ from Figure 5, by taking the B2 KCl parameters from Table 1, and by computing O_2 volume by difference between the phase volumes at each temperature as a function of pressure. These isotherms are fit with a thermal *Birch* [1986] EOS, the parameters of which are listed in the figure and in Table 1. V_o^* is the fictive volume that O_2 would have if it behaved as a condensed phase to ambient, which, of course, it does not. It is used as a convenience in fitting the EOS for O_2 in the P-T region we investigate where O_2 is a supercritical condensed fluid. [Fitting condensed fluid isotherms with V_o^* is exactly analogous to fitting for V_o in the case of R $KClO_3$ or B2 KCl, which cannot be recovered for direct measurement at ambient. The difference is that the unrecoverable condensed O_2 fluid has no phase change with the gas that is recovered.] The isotherms smooth the expected variation by fitting on all the $KClO_4$ and KCl data at all P and T. The individual points are computed from specific pairs of phase volume data from the tables. Fitting on the points themselves makes very little difference to the extrapolations of this data used in Figure 1, even though the K_o and K_o' numbers covary antithetically by about a factor of 2. The global fit does little violence to the individual data points. The whole range of temperatures cannot all satisfy the Clausius–Clapeyron equation because at each pressure there will only be a single equilibration temperature for (4). Thus, the rigorous O_2 volume can be computed at only one T at each P. However, the calculation of O_2 volume is very insensitive to the T chosen because the thermal expansions of the phases are very similar to each other and the T range is small. Part (b) shows the volume of O_2 computed for several other data sets. The isotherms from part (a) are also shown. The $KClO_4$-KCl 1997 data set has not been previously reported but was collected in the study of *Johnson et al.* [2001]. Although these other studies are of lower precision than the present one, for well-understood reasons, the mutual agreement is gratifying. Conventionally accepted O_2 volumes used in the calculations of Figure 1a plot off the top of this diagram because the discrepancy is so large. In contrast, the five different data sets on three different compounds show good internal agreement here.

[27] Unfortunately it is not yet possible to resolve all inconsistencies surrounding the present issues. The DAC observations of reaction (1) successfully proceeding at more than 300 kbar, the new O_2 volume measurements based on chlorate equilibria, and the phase equilibria-based prediction of high solubility of O_2 in liquid metal at high pressure [*Ohtani et al*, 1984] are all mutually consistent. On the other hand, shock wave [*Nellis and Mitchell*, 1980] and ISS [*Abramson et al.*, 1999] measurement of fluid O_2 volumes do not encourage the view that much O_2 should dissolve in liquid metal at high pressure. Solubility measurement of O_2 in liquid metal by *O'Neill et al.* [1998] and *Ito et al.* [1995] reinforce the expectation of poor solubility.

8. Oxygen Volume Discrepancies

[28] The first discrepancy to address is that of the O_2 volume measurements between the chlorate-based and dynamic techniques. The chlorate measurements are indirect and depend upon the decompositions being equilibria. If they are, then the Clausius–Clapeyron equation applies. We compute O_2 volumes by approximation from the difference between solid products and reactants without any entropy corrections from the low $\partial T/\partial P$ slope. This is necessary because the entropy of B2 KCl is unknown. *Johnson et al.* [2001] pointed out that the O_2 volume calculations are very insensitive to the approximation of ignoring the entropy correction even for extreme possible choices of phase entropy. Probable errors were implausibly as large as 5% whereas the discrepancy to be understood approaches 50%. Furthermore the fact that the results from R $KClO_3$, O $KClO_4$, and T $RbClO_4$ all agree with one another so well even though they have slightly different decomposition slopes indicates that resolution is unlikely from this direction.

[29] Another potential error in our calculation is that the stoichiometry of the $KClO_3$ and $KClO_4$ phases may deviate from integer at high pressure and temperature. The oxygen volumes we compute are sensitive to the actual amount of O_2 in the various chlorates. For instance, if KCl-buffered $KClO_4$ has less than 4 oxygen, then the ${}^{O_2}\overline{V}$ we compute on the assumption that it is $KClO_4$ that we are decomposing will be too small. The real ${}^{O_2}\overline{V}$ would be larger. To remove the discrepancy between our $KClO_4$ data and the dynamic techniques, $KClO_4$ would need to actually have less O_2 than $KClO_3$. Because we observed $KClO_3$ to disproportionate to $KClO_4$ with the liberation of excess KCl, this resolution does not appear possible. Furthermore $KClO_4$ recovered from high P-T gives XRD patterns indistinguishable in cell parameters from known stoichiometric $KClO_4$. ($KClO_4$ is the only one of the three chlorates studied that exists at high P-T and can be quenched from P-T in the same structure as at ambient. Thus this check on stoichiometry is not available for the quenched products of R $KClO_3$ and T $RbClO_4$ we have examined in alternate studies.) And all three chlorates give the same value for ${}^{O_2}\overline{V}$ within error, and this volume is very different from the dynamic measurements. It is unlikely that all three phases would have the exactly the same nonstoichiometry and thereby provide a viable resolution to the discrepancy.

[30] Yet another possible resolution could be with regard to the timescale of the equilibrations involved. The shock state measurements explore a timescale of microseconds whereas ours explore a timescale of 10s of minutes. It is tempting to argue that the chlorate-based results are therefore more informative about longer-term stabilities and solubilities. This temptation will be resisted because the long-term measurements of solid O_2 volumes to 100 kbar give values slightly *larger* than our fluid volumes [*Schiferl et al.*, 1983]. Our small, chlorate-based fluid volumes are therefore difficult to reconcile with the observed positive Clapeyron slope for the O_2 melting curve measured with long-term experiments [*Desgreniers et al.*, 1990; *Abramson et al.*,1999]. The shock wave and ISS measurements do not suffer from this discrepancy because their fluid volumes are larger than the solids, even though the measurement timescales are very short. Besides, appealing to a timescale resolution begs the question as to what change, to which phases, drives the differing behaviors on different timescales. The solid phases are not observably altering their XRD character.

This suggests that it might be changes in the fluid phase with time which are responsible for the discrepancies between timescales. But it is the fluid properties such as volume which are the focus of the investigation, so it is unhelpful to claim the discrepancies are a consequence of the desired observations being a moving target with change of timescale. That would be just a convoluted restatement that a discrepancy exists. Although it may or may not be true that timescale issues are at the root of the problem, this potential resolution currently provides little insight because of the absence of a structural mechanistic explanation of what changes with time.

[31] The O_2 fluid volumes from shock wave and ISS have pressure and density as the best-determined parameters but at temperatures that are not directly measured. *Ross and Ree* [1981] have given estimates of temperature along the oxygen Hugoniot which approach 25,000 K at a megabar, but are only $\sim$2000 K at the pressures of immediate interest for comparison to the chlorate results. Therefore direct comparison requires extra manipulation. MD reparameterization of these shock wave results give much higher volumes than chlorate-based at the same P,T. It is not clear to what extent thermal shock perturbations affect the ISS results but they agree well with the shock and MD methods. However, our chlorate-based determinations are taken $\sim$350$-$600°C higher in temperature than the ISS results, so it is possible that structural transitions or negative thermal expansion within the fluid O_2 phase could rationalize the disparate results. This highly conjectural resolution may make it seem more attractive to simply discount one set of results as in error, somehow undiscovered. But which set?

[32] Let us suppose that we reject the chlorate-based numbers as truly giving the volume of fluid oxygen for reasons presently not understood. The numbers do not go away. There is virtually no way they can be in significant numerical error because the volumes of the diffracting solid phases are well determined and the results are consistent across a collection of several phases. What then do these volumes represent if not that of fluid oxygen? Formally the difference between the product and reactant solid volumes gives the partially molar volume of O_2 in the chlorate/chloride assemblage whether or not it is also the volume of fluid oxygen. And it is the partial molar volumes rather the volumes of fluids themselves which are of interest in determining issues like solubility. Although a solid chloride/chlorate assemblage is not liquid metal, our O_2 volume numbers are relevant to solubility issues whether or not they might or might not be the volume of fluid oxygen. Thus the discrepancy with other measurements of fluid O_2 volumes becomes an interesting sideshow rather than an insurmountable obstacle to estimating the capacity of the core for absorbing O_2.

[33] We note with interest the recent report of *Benedetti* [2001] of a new solid phase of O_2 whose volume has been measured by XRD between 0 and 46 GPa and is very comparable to, but slightly smaller than, our fluid O_2 volumes. If confirmed, this discovery would remove several of the obstacles to accepting our results as plausible. The issue would then become one of determining whether the dense fluid (and solid) phases of O_2 that we favor are more stable or less stable than those investigated previously by dynamic techniques.

9. Oxygen Solubility Discrepancy

[34] The second discrepancy to address is the one between DAC observations and the MA solubility measurements. DAC indications of forward progress in reaction (1) with pressure above 300 kbar require increasing oxygen solubility in liquid metal. But solubility measurements to 250 kbar indicate little such solubility. One possible resolution is that the solubility measurements to 250 kbar simply have not gone to high enough pressure. However, the solubility measurements of *O'Neill et al.* [1998] indicating *decreasing* solubility with pressure are also discrepant with the modest pressure work of *Ohtani et al.* [1984] indicating increasing solubility with pressure. Ohtani et al. did not measure solubility but inferred it by comparing the rate of rise of the Fe melting point with that of the eutectic temperature. The eutectic *E* in Figure 2 is between crystalline metal and oxide where liquid metal is the eutectic phase. They

interpreted the more rapid rise of the Fe melting point than the temperature of the eutectic with pressure from 0 to 40 kbar as an indication that the eutectic composition should become more O_2-rich with pressure. Because the eutectic temperature increases with pressure so should O_2 solubility as shown in Figure 2.

[35] A particularly robust aspect of the Ohtani et al. work is that the DTA determinations are not vulnerable to quench problems. Quenching is an admitted weakness of the *O'Neill et al.* [1998] cook, look, and analyze approach. O_2 may be lost from the quenched products of what was liquid metal alloy at experimental *P* and T. O'Neill et al. were very careful to document and avoid their observable quench effects. They may not have been entirely successful in this avoidance effort. A curious aspect of their data is that they show substantial increases in O_2 solubility with temperature from 1800°C to 2200°C but none beyond that. Rather than acknowledge that this data structure is an artifact of quenching, they dismissed their 2400°C/90 kb data point as anomalous and interpreted their 2500°C, 250 kb data point's static O_2 solubility as a consequence of a decrease in solubility with pressure offsetting the increase with temperature. This interpretation is permissible in the context of their 2200°C data points at 180 and 220 kbar which show less O_2 solubility than their 2200°C points at 80 and 90 kbar. However, it appears equally plausible to us that the relatively static values of $\ln([O]_{met}/[FeO]_{ox})$ at 2200°C and above result from the inability of the charges to effect closure to O_2 until the temperature during quench falls to $\sim$2200°C. The variation in O_2 in metal at 2200°C with pressure could represent a decreasing temperature of closure with increasing pressure. This reinterpretation can be sustained because diffusion distances are about half as long in the smaller charges used by O'Neill et al. at high P, and therefore the charges are more vulnerable to diffusive nonclosure. Given the scale of the area affected by diffusive quenching effects shown for their larger 90 kbar charges, it is difficult to imagine that the half-sized charges at higher pressures (not shown) could have escaped closure damage.

[36] An additional contributory circumstance may be that diffusion becomes more rapid at high pressure. More rapid diffusion with higher pressure in liquid metal solutions is conjectural but is consistent with substantial increases in Fe-S diffusivity with pressure observed in this lab. *Majewski and Walker* [1998] were able to resolve the risetime for Fe-S Soret diffusive redistribution at 10 kb and to quantitatively determine $D \sim 10^{-5}$ cm^2/s at 1450°C. However, subsequent efforts to measure the diffusivity at 100 kb have failed because the risetime for the effect is too rapid to resolve in a time series. Similar non-Stokes–Einstein behavior may apply to Fe-O. Even if Fe-O diffusion is not more rapid at high pressure, O'Neill et al.'s results are understandable in terms of quench-closure problems being more severe in smaller high-pressure charges. This reinterpretation allows inclusion of the 2400°C data point they were forced to exclude in their interpretation. Consequently we believe the case for decreasing O_2 solubility with pressure is less secure than the case for increasing solubility with pressure. No solubility discrepancy exists if the *O'Neill et al.* [1998] data is reinterpreted in a way so as to include all their data.

10. Implications for D″

[37] The reaction of (1) is found experimentally to proceed at $\boldsymbol{P} > 300$ kbar and this pressure of transition between reaction and no-reaction is consistent with the new oxygen volume measurements. But the core mantle boundary interface across which the outer core Fe alloy and lower mantle Fe-bearing silicates and oxides might interact is roughly a megabar higher in pressure. This leads to Knittle and Jeanloz's interpretation that the core–mantle interface is one of violent reaction promoted by high pressure rather than the equilibrium expected at $\sim$300 kbar. In their interpretation D″ forms as a result of

$$^{liq}\mathrm{Fe} + (\mathrm{MgFe})\mathrm{pvsk} = \mathrm{Mgpvsk} + \mathrm{SiO_2} + {}^{liq}\mathrm{Fe} + {}^{liq}\mathrm{FeSi} + {}^{liq}\mathrm{FeO} \qquad (6)$$

Silica, Fe-poor perovskite (and possibly iron silicide) accumulate at the interface and become the constituents of D″. (We dispute their suggestion that FeO would accumulate in D″ because it is the solution of FeO into Fe liquid of the core, which drives the reaction.) The D″ reaction is a pump, which puts oxygen into the core. Virtually all the material accumulating in D″ is derived from the mantle, not the core, and so this reaction should be an effective seal to sequester siderophile material in the core. The core is gradually trying to reach an accommodation with the mantle by either absorbing a saturating amount of FeO (and maybe FeSi) or else by insulating itself with a D″ corrosion product.

[38] In order for such a gross disequilibrium situation to have been set up between the core and mantle, the initial core formation process must either have been by heterogeneous accretion or else by a low-pressure smelting process producing core metal. For the low pressure smelting scenario, rapid delivery of the material to the Earth's center without an opportunity to react with lower mantle silicate and oxide is needed. Upper-mantle-deep terrestrial magma oceans [*Li and Agee*, 1996; *Righter et al.*, 1997] are suitable vessels in which to produce core metal which catastrophically drained to the Earth's center. This scenario is viable and is consistent with the picture of the core's long-term evolution toward oxygen saturation being frustrated by the need to communicate chemically across the D″ layer of waste products of the reaction pumping oxygen to the core.

[39] However if core metal remains in contact with its slag at P > 300 kbar or if core-forming Fe alloy is slowly delivered to the Earth's center [*Minarik et al.*, 1996] across the lower mantle at $P > 300$ kbar, then reactions (1) and (6) will operate. Saturation of the core with oxygen would be expected as suggested by *Stevenson* [1988]. *Ito et al.* [1995] have embraced this scenario and have pointed out that core cooling over time and crystallization of the inner core should lead to supersaturation of the outer core. In their model, supersaturation leads to exsolution of blobs of Fe-O-Si liquid which accumulate and crystallize to form D″. *Buffet et al.* [2000] produced a variant of this model in which the upward sedimentation of oxygen-rich material exsolving from the core is crystalline oxide/silicate. In general terms they are proposing that a high-temperature liquid analog of reaction (6) runs backward as the core evolves, rather than forward. This prediction is reasonable assuming that the core reached saturation at some point in its earlier history. This core evolution from supersaturation scenario appears at least as viable as Knittle and Jeanloz's, but it is important to note that material transfer is no longer strictly into the core. In fact Fe and presumably other siderophile elements are being pumped back into the oxide part of the Earth. The core is no longer an oxygen sink, but is already oxygen-saturated with reactions like (1) and (6) returning oxygen and siderophile elements, including Fe, from the core to the mantle's D″ base.

[40] It might be possible to choose between these two scenarios if it were known whether or not material from the Earth's core was being returned to the mantle. *Walker et al.* [1995, 1997] and *Brandon et al.* [1998] have made a case from the coupled ^{186}Os and ^{187}Os anomalies seen in some plume-related basic volcanic rocks that such a return flux is being seen. They conclude that a small proportion of the highly siderophile elements (HSE) contained in some parts of the Siberian and Hawaiian plumes contain material derived from the outer core.

[41] Slight fractionation of Os from Re and extensive fractionation of Os from Pt is needed to explain the correlated Os isotope anomalies. Growth of the inner core from the outer core is expected to produce these sorts of fractionations, at least qualitatively, based upon study of IIa iron meteorite fractionation trends [*Pernicka and Wasson*, 1987; *Morgan et al.*, 1995]. Experiments [*Fleet et al.*, 1991, 1999; *Walker*, 2000] on Pt Re Os fractionation between liquid and solid metal at pressures up to 100 kbar strongly support the notion that inner core growth would impart a semiquantitatively correct signal to the outer core. It remains to be shown conclusively that this is the only way in which the correlated Os anomalies could be produced. However, if it is concluded from Os studies that the core really is still participating in mantle geochemistry, the D″ reaction running in reverse from a supersaturated core provides a plausible delivery mechanism for reimplanting the Os signal (and other HSE) back into

the mantle. Operation of such a siderophile element pump may also be a key to the solution of some of the remaining siderophile element abundance and relative fractionation anomalies in the mantle.

[42] Studies most urgently needed to clarify these issues are ones to determine the solubility of FeO in molten Fe at greater-than-megabar pressures and ones to decide if the Os signal could come from somewhere other than the core.

Acknowledgments

[43] This work was supported by the UK Natural and Environmental Research Council, CLRC Daresbury Laboratory, and the US National Science Foundation. We have benefited from the EPSRC-funded CCP14 project at http://www.ccp14.ac.uk. We thank R. J. Walker, R. Boehler, E. Cottrell, A. Kavner, and B. Scott for helpful insights and discussion. We thank G. Harlow, E. Mathez, and M. Walter for comments on earlier versions of this work and D. Stevenson and an anonymous reviewer for their comments on the present manuscript. We thank L. R. Benedetti for sharing her results in advance of publication. Lamont-Doherty Earth Observatory contribution 6377.

References

Abramson, E. H., L. J. Slutsky, M. D. Harrell, and J. M. Brown, Sound speed and equation of state for fluid oxygen to 10 GPa, *J. Chem. Phys.*, *110*, 10,493–10,497, 1999.

Barnes, P., A. C. Jupe, S. L. Colston, S. D. Jacques, A. Grant, T. Rathbone, M. Miller, S. M. Clark, and R. J. Cernik, A new three angle energy-dispersive diffractometer, *Nucl. Instrum. Methods Phys. Res.*, *134*, 310–313, 1998.

Belonoshko, A., and S. K. Saxena, A molecular dynamics study of the pressure–volume–temperature properties of supercritical fluids, II, CO_2, CH_4, CO, O_2, and H_2, *Geochim. Cosmochim. Acta*, *55*, 3191–3208, 1991.

Benedetti, L. R., Molecular systems at high pressures and temperatures: Solar system astronomy in a physics laboratory, Ph.D. thesis, Physics Dept., Univ. of Calif., Berkeley, 2001.

Birch, F., Equation of state and the thermodynamic parameters of NaCl to 300 kbar in the high-temperature domain, *J. Geophys. Res.*, *91*, 4949–4954, 1986.

Boehler, R., and G. C. Kennedy, Equation of state of sodium chloride up to 32 kbar and 500°C, *J. Phys. Chem. Solids*, *41*, 517–523, 1980.

Boehler, R., N. von Bargen, and A. Chopelas, Melting, thermal expansion, and phase transitions of iron at high pressures, *J. Geophys. Res.*, *95*, 21,731–21,736, 1990.

Brandon, A. D., R. J. Walker, J. W. Morgan, M. D. Norman, and H. M. Prichard, Coupled ^{186}Os and ^{187}Os evidence for core–mantle interaction, *Science*, *280*, 1570–1573, 1998.

Buffett, B. A., E. J. Garnero, and R. Jeanloz, Sediments at the top of Earth's core, *Science*, *290*, 1338–1342, 2000.

Campbell, A. J., and D. L. Heinz, Compression of KCl in the B2 structure to 56 GPa, *J. Phys. Chem. Solids*, *52*, 495–499, 1991.

Chase, M. W., Jr., NIST-JANAF thermochemical tables, fourth edition, *J. Phys. Chem. Ref. Data Monogr.*, *9*, 1–1951, 1998.

Clark, S. M., A new energy dispersive powder diffraction facility at the SRS, *Nucl. Instrum. Methods Phys. Res., Sect. A*, *381*, 161–168, 1996.

Cohelo, A. A., and R. W. Cheary, X-ray line profiling program, XFIT, Internet distributed freeware, (Available at http://www.ccp14.ac.uk), 1997.

Decker, D. L., High-pressure equation of state for NaCl, KCl, and CsCl, *J. Appl. Phys.*, *42*, 3239–3244, 1971.

Desgreniers, S., Y. K. Vohra, and A. L. Ruoff, Optical response of very high density solid oxygen to 132 GPa, *J. Phys. Chem.*, *94*, 1117–1122, 1990.

Fei, Y., H.-K. Mao, J. Shu, and J. Hu, P-V-T equation of state of magnesiwũstite ($Mg_{0.6}Fe_{0.4}$)O, *Phys. Chem. Miner.*, *18*, 416–422, 1992.

Fleet, M. E., R. Tronnes, and W. E. Stone, Partitioning of PGE in the Fe-O-S system to 11 GPa and their fractionation in the mantle and meteorites, *J. Geophys. Res.*, *96*, 21,949–21,958, 1991.

Fleet, M. E., M. Liu, and J. H. Crocket, Partitioning of trace amounts of highly siderophile elements in the Fe-Ni-S system and their fractionation in nature, *Geochim. Cosmochim. Acta*, *63*, 2611–2622, 1999.

Fritz, J. N., S. P. Marsh, W. J. Carter, and R. G. McQueen, The Hugoniot equation of state of sodium chloride in the sodium chloride structure, in *Accurate Characterization of the High Pressure Environment, NBS Spec. Publ.*, *326*, edited by E. C. Lloyd, pp. 201–208, 1971.

Goarant, F., F. Guyot, J. Peyronneau, and J.-P. Poirier, High-pressure and high-temperature reactions between silicates and liquid iron alloys, in the diamond anvil cell, studied by analytical electron microscopy, *J. Geophys. Res.*, *97*, 4477–4487, 1992.

Hazen, R. M., and R. Jeanloz, Wũstite ($Fe_{1-x}O$): A review of its defect structure and physical properties, *Rev. Geophys.*, *22*, 37–46, 1984.

Heinz, D. L., and R. Jeanloz, Measurement of the melting curve of $Mg_{0.9}Fe_{0.1}$SiO3 perovskite at lower mantle conditions and its geophysical implications, *J. Geophys. Res.*, *92*, 11,437–11,444, 1987.

Hofmeister, A. M., IR spectroscopy of alkali halides at very high pressures: Calculation of equations of state and the response of bulk moduli to the B1–B2 phase transition, *Phys. Rev. B*, *56*, 5835–5855, 1997.

Holland, T. J. B., and S. A. T. Redfern, Unit cell refinement from powder diffraction data: The use of regression diagnostics, *Mineral. Mag.*, *61*, 65–77, 1997.

Hunter, B., Rietica: A visual Rietveld program, Int. Union of Crystallogr. Com. on Powder Diffr. Newsletter 20 (Summer), 1998. (Available at http://www.rietica.org)

Ito, E., K. Morooka, O. Ujike, and T. Katsura, Reactions between molten iron and silicate at high pressure: Implications for the chemical evolution of the Earth's core, *J. Geophys. Res.*, *100*, 5901–5910, 1995.

Johnson, M. C., D. Walker, S. M. Clark, and R. L. Jones, Rhombohedral $KClO_3$ decomposition: O_2 gas volumes at 36–76 kbar, *Eos Trans. AGU*, *78*, S313, 1997.

Johnson, M. C., D. Walker, S. M. Clark, and R. L. Jones, Thermal decomposition of rhombohedral $KClO_3$ from 29–76 kilobars and implications for the molar volume of fluid oxygen at high pressures, *Am. Mineral.*, *86*, 1367–1379, 2001.

Knittle, E., and R. Jeanloz, Simulating the core–mantle boundary: An experimental study of high-pressure reactions between silicates and liquid iron, *Geophys. Res. Lett.*, *16*, 609–612, 1989a.

Knittle, E., and R. Jeanloz, Melting curve of $(Mg,Fe)SiO_3$ perovskite to 96 GPa: Evidence for a structural transition in lower mantle melts, *Geophys. Res. Lett.*, *16*, 421–424, 1989b.

Knittle, E., and R. Jeanloz, Earth's core-mantle boundary: Results of experiments at high pressures and temperatures, *Science*, *251*, 1438–1443, 1991.

Le Bail, A., H. Duroy, and J. L. Fourquet, Ab-initio structure determination of $LiSbWO_6$ by X-ray powder diffraction, *Mater. Res. Bull.*, *23*, 447–452, 1988.

Li, J., and C. B. Agee, Geochemistry of mantle–core differentiation at high pressure, *Nature*, *381*, 686–689, 1996.

Majewski, E., and D. Walker, S diffusivity in Fe-Ni-S-P melts, *Earth Planet. Sci. Lett.*, *160*, 823–830, 1998.

Minarik, W. G., F. J. Ryerson, and E. B. Watson, Textural entrapment of core-forming melts, *Science*, *272*, 530–533, 1996.

Morgan, J. W., M. F. Horan, R. J. Walker, and J. N. Grossman, Rhenium–osmium concentration and isotopic systematics in group IIAB iron meteorite, *Geochim. Cosmochim. Acta*, *59*, 2331–2344, 1995.

Nellis, W. J., and A. C. Mitchell, Shock compression of liquid Ar, N_2 and O_2 to 90 GPa, *J. Chem. Phys.*, *73*, 6137–6145, 1980.

Ohtani, E., A. E. Ringwood, and W. Hibberson, Composition of the core, II, Effect of high pressure on solubility of FeO in molten iron, *Earth Planet. Sci. Lett.*, *71*, 94–103, 1984.

O'Neill, H. St. C., D. Canil, and D. C. Rubie, Oxide–metal equilibria to 2500°C and 25 GPa: Implications for core formation and the light component in the Earth's core, *J. Geophys. Res.*, *103*, 12,239–12,260, 1998.

Pernicka, E., and J. T. Wasson, Ru, Re, Os, Pt and Au in iron meteorites, *Geochim. Cosmochim. Acta*, *51*, 1717–1726, 1987.

Righter, K., M. J. Drake, and G. Yaxley, Prediction of siderophile element metal/silicate partition coefficients to 20 GPa and 2800°C: The effects of temperature, pressure, oxygen fugacity, and silicate and metallic melt compositions, *Phys. Earth Planet. Inter.*, *100*, 115–134, 1997.

Ross, M., and F. H. Ree, Repulsive forces of simple molecules and mixtures at high density and temperature, *J. Chem. Phys.*, *73*, 6146–6152, 1980.

Schiferl, D., D. T. Cromer, L. A. Schwalbe, and R. L. Mills, Structure of "orange" $^{18}O_2$ at 9.6 GPa and 297 K, *Acta Crystallogr.*, *B39*, 153–157, 1983.

Smith, M., and S. Gontier, *DLConverter for Windows 95/NT*, CLRC Daresbury Lab., Cheshire, UK, 1999. (Available at http://www.ccp14.ac.uk/projects/dl-conv/)

Stevenson, D. J., Infiltration, dissolution and underplating: Rules for mixing core–mantle cocktails, *Eos Trans. AGU*, *69*, 1404, 1988.

Vaidya, S. N., and G. C. Kennedy, Compressibility of 27 halides to 45 kbar, *J. Phys. Chem. Solids*, *32*, 951–964, 1971.

Wackerle, J., W. L. Seitz, and J. C. Jamieson, Shock-wave equation of state for high density oxygen, in *Behavior of Dense Media under High Dynamic Pressure*, 563 pp., Gordon and Breach, Newark, N. J., 1968.

Walker, D., Core participation in mantle geochemistry: Geochemical Society Ingerson Lecture, GSA Denver, October 1999, *Geochim. Cosmochim. Acta*, *64*, 2897–2911, 2000.

Walker, D., C. B. Agee, and Y. Zhang, Fusion curve slope and crystal/liquid buoyancy, *J. Geophys. Res.*, *93*, 313–323, 1988.

Walker, D., S. M. Clark, R. L. Jones, and L. M. D. Cranswick, Rapid methods for the calibration of solid state detectors, *J. Synchrotron Radiat.*, *7*, 18–21, 2000.

Walker, D., G. Hughes, L. M. D. Cranswick, S. M. Clark, and S. Buhre, Synthesis and thermal decomposition of tetragonal $RbClO_4$ and volume of fluid oxygen from 2–9 GPa, *Geochem. Geophys. Geosyst.*, *2*, doi:10.1029/2001GC000154, 2001.

Walker, D., L. M. D. Cranswick, P. K. Verma, S. M. Clark, and S. Buhre, Thermal equations of state for B1 and B1 KCl, *Am. Mineral.*, *87*, 805–812, 2002.

Walker, R. J., J. W. Morgan, and M. F. Horan, ^{187}Os enrichment in some plumes: Evidence for core–mantle interaction, *Science*, *269*, 819–822, 1995.

Walker, R. J., J. W. Morgan, M. I. Smoliar, E. Beary, G. K. Czamanske, and M. F. Horan, Applications of the ^{190}Pt–^{186}Os isotope system to geochemistry and cosmochemistry, *Geochim. Cosmochim. Acta*, *61*, 4799–4808, 1997.

Yagi, T., Experimental determination of thermal expansivity of several alkali halides, *J. Phys. Chem. Solids*, *39*, 563–571, 1978.

Yagi, T., T. Suzuki, and S. Akimoto, Static compression of Wũstite ($Fe_{0.98}O$) to 120 GPa, *J. Geophys. Res.*, *90*, 8784–8788, 1985.

Zerr, A., and R. Boehler, Melting of $(Mg,Fe)SiO_3$-perovskite to 625 kilobars: Indication of a high melting temperature in the lower mantle, *Science*, *262*, 553–555, 1993.